In presenting this thesis in partial fulfillment of the requirements for an advanced degree at Idaho State University, I agree that the Library shall make it freely available for inspection. I further state that permission to download and/or print my thesis for scholarly purposes may be granted by the Dean of the Graduate School, Dean of my academic division, or by the University Librarian. It is understood that any copying or publication of this thesis for financial gain shall not be allowed without my written permission.

Signature _____

Shawn Craig Seegmiller

Date _____

SENSITIVITY ANALYSIS OF THE EXPERIMENTAL BREEDER REACTOR II

by

Shawn Craig Seegmiller

A thesis

submitted in partial fulfillment

of the requirements for the degree of

Master of Science in Nuclear Science and Engineering

Idaho State University

August 2015

To the Graduate Faculty:

The members of the committee appointed to examine the thesis of Shawn Seegmiller find it satisfactory and recommend that it be accepted.

_____

Dr. Chad Pope,

Major Advisor

_____

Dr. Jay Kunze,

Committee Member

_____

Dr. Seyed Mousavinezhad,

Graduate Faculty Representative

Dedication

This thesis is dedicated to the many scientists and engineers who labored diligently to make the integral fast reactor a reality.

Acknowledgements

I would like to begin by acknowledging my professor, Dr. Chad Pope, for the patient mentoring he has given me throughout my research. Additionally, I would like to thank Dr. Jay Kunze for his encouragement and guidance in helping me to pursue a nuclear engineering degree. I would also like to thank Dr. Charles Till and Dr. Yoon IL Chang, whose writings inspired me to go into the nuclear industry in the first place, for their key roles in the development of the integral fast reactor, upon which this thesis is based. A special acknowledgement goes out to the memory of Dr. Michael Lineberry and Dr. Leonard Koch, both of whom contributed greatly to the IFR project.

Finally, I would like to give my heartfelt thanks to my wife Ruth for supporting me in my schooling despite the long hours away from home.

VITA

Shawn Seegmiller was born on May 29, 1989 in St. George, Utah. After completing his Associate of Science degree from Dixie State College he attended Brigham Young University – Idaho where he earned his Bachelor's degree in Mechanical Engineering. During this time he had the privilege of interning at a solenoid valve manufacturing facility called RAM Company in his hometown of St. George, as well as the auto manufacturer BMW in Leipzig, Germany. Upon finishing at BYU-Idaho he was accepted into the Master's program of Nuclear Science and Engineering at Idaho State University. He currently works as an engineer for Arizona Public Service at Palo Verde Nuclear Generating Station.

Table of Contents

LIST OF FIGURES

LIST OF TABLES

Abstract

The goal of this project was to perform a sensitivity analysis on the Experimental Breeder Reactor II. The results of the analysis contribute to a reactor physics benchmark of the reactor, suitable for inclusion in the International Reactor Physics Experiment Evaluation Project (IRPhEP) handbook. The analysis was performed by creating a computer model of EBR-II, and perturbing various nuclide cross sections and material densities to determine the individual effect on the reactor multiplication factor (k-eff). Software used for the analysis included KENO and TSUNAMI, both a part of the SCALE package distributed by Oak Ridge National Laboratory. The results show that k-eff is most sensitive to U-235 nubar($\overline{\nu}$) with a sensitivity coefficient of 0.96081, followed closely by the U-235 fission and total cross sections, with sensitivity coefficients of 0.52769 and 0.4581 respectively. Taking the cross section covariance data into account, the greatest contributor to overall uncertainty was the U-235 (n,gamma) cross section, with an uncertainty contribution of 2.1777 % Δk/k. The material density that had the greatest effect on k-eff was that of the enriched uranium fuel mixture, with a sensitivity coefficient of 0.46387. These results help reactor physicists know what to concentrate on when improving a computer model of the EBR-II and cross section measurements.

Chapter 1: Introduction

Since the first successful demonstration of a sustained nuclear chain reaction in Chicago in 1942, many different types of nuclear reactors have been built and operated. In 2013 nuclear power supplied about 19% of electricity produced in the United States [1]. As knowledge in areas of nuclear science and engineering has advanced, the complexity and accuracy of computational methods has increased, to the point that it is now possible to perform many different reactor calculations using 3D computer models. With computer codes becoming widely used computational tools, the validation of these codes has taken a high priority. One approach to code validation involves the use of reactor physics benchmarks. This requires comparing calculated values with actual reactor measurements to see how well they compare [2]. One difficulty in using benchmark validation is the necessity to quantify uncertainties associated with both the calculations as well as the measurements. To assist in quantifying these uncertainties, a sensitivity analysis can be performed. A sensitivity analysis is able to determine the degree to which small adjustments in individual neutron cross sections and material densities affects a reactor criticality calculation [3].

A specific reactor called the Experimental Breeder Reactor II (EBR-II), was chosen as a desirable candidate for a reactor physics benchmark due to its unique features and capabilities. In connection with the benchmark, the goal of this project was to perform a sensitivity analysis on the EBR-II. The purpose of this thesis is to explain more fully what a benchmark is and how it is used, describe the EBR-II and its significance, clarify

what a sensitivity analysis is and how it is performed, describe the computer model that was created for this purpose, and present the analysis results along with their importance.

Chapter 2: Benchmarking

The overarching purpose of the sensitivity analysis was to contribute to a reactor physics benchmark of the EBR-II, suitable for inclusion in the International Reactor Physics Experiment Evaluation Project (IRPhEP) handbook.

A benchmark can be defined as a standard against which similar things are measured [8]. In the case of nuclear reactor physics, a benchmark gives computer code developers a standard against which they can compare the outputs of their code [2]. Creating a reactor physics benchmark begins with the gathering of data about an actual nuclear reactor. Such data will include geometry specifications such as fuel rod diameter and height, or cladding thickness. It must also include material specifications such as the composition for the fuel, cladding, and coolant along with their respective densities. Nominal data however is not enough, everything comes with a degree of uncertainty, and this uncertainty must be quantified [9]. To demonstrate with an example, it may be known that the fuel rod height for a hypothetical reactor is 60 centimeters, with an uncertainty of ± 0.5 centimeters due to irradiation induced swelling. Once geometry and material data are gathered, and associated uncertainties are quantified, a computer model is created which represents the actual reactor as closely as possible. At this point, it must be decided what values are actually to be benchmarked. For example, it may be decided to benchmark the control rod positions to achieve criticality. In this case, more information will be needed about the actual reactor, such as critical control rod positions with corresponding neutron detector count

rates and reactor temperature [9]. These too would have associated uncertainties. The computer model would then be established to have the same control rod positions, and the effective multiplication factor (k-eff) would be calculated. Computer code calculations also come with uncertainties. At this point it would also need to be determined how the uncertainty in the geometry and material data impacts the calculated value for k-eff. The final results might look similar to those below [2]:

Calculated Value	Benchmark Value
k-eff = 1.003 ± 0.002	k-eff = 1.001 ± 0.001

The above hypothetical results would indicate that with uncertainties included, the calculated value for k-effective matches that of the benchmark value. This in turn helps validate the computer code.

Some possible reactor physics measurements to be evaluated for the EBR-II benchmark include approach to critical measurements, critical configuration measurements, reactor scram measurements, and reactor physics measurements related to safety tests and transient overpower tests [9]. These would then be included in the IRPhEP handbook.

The goal of the IRPhEP handbook is to preserve data from past reactor physics experiments, so that other reactor physicists can validate their own calculation techniques [2]. Data from numerous different reactors are included, from many countries around the world. These are extensively peer reviewed and compiled into a

standardized format. The inclusion of an EBR-II benchmark would be a valuable addition to the collection, as further explained in the next chapter.

Chapter 3: Experimental Breeder Reactor II

The Experimental Breeder Reactor II, commonly known as the EBR-II, was a pool type, sodium cooled, metal fueled, fast neutron spectrum reactor [4]. Pool type refers to the large pool of molten sodium metal in which the reactor resided, which was pumped through the reactor for cooling. Because sodium does not provide for significant moderation, the majority of the neutron population retained their initial high kinetic energies. The fuel, rather than being made from uranium dioxide (typical of most commercial reactors), was in metallic form. Details of the metal alloy are discussed below. The reactor operated from 1964 through 1994 and had a maximum heat output of 62.5 MW, which in turn was used to produce around 20 MW of electricity [4] [5]. Although initially designed to breed more fuel than it consumed, EBR-II was later reconfigured to operate as an irradiation facility where a variety of fuels and structural materials were tested [6].

The EBR II consisted of 637 vertical, hexagonally shaped, removable subassemblies. These were divided into three regions (moving outward from the middle): the core, an inner blanket, and an outer blanket [5]. The number of subassemblies within each region varied over the years with changing configurations, due to the experimental nature of the reactor [6]. Located in the core region were driver subassemblies containing 91 fuel rods each. In the EBR-II a fuel rod was also called a fuel “element.” The fuel was made of enriched uranium metal, alloyed with a small percentage of other elements to improve fuel properties, and clad within stainless

steel tubes [7]. Also in the core region were two safety and eight control subassemblies [6] [7]. Both the safety and control subassemblies contained 61 fuel elements, and could be inserted to increase reactor power, or lowered from the core to reduce the reactor power [7]. The control rods were later upgraded to a high worth version, which included a B_4C poison region above the fuel in order to maximize the reactivity swing [6]. Other subassemblies in this region included stainless steel dummies, half worth drivers, and experimental/instrumentation subassemblies [7]. The inner blanket region initially consisted of subassemblies which contained depleted uranium, for the purpose of breeding fissile material, as well as reflecting neutrons back toward the center of the core. After proving the breeding concept, these were replaced with stainless steel reflectors more compatible with the goal of an irradiation facility. The outer blanket region consisted almost entirely of depleted uranium subassemblies, again for breeding and reflection [6]. These were maintained as depleted uranium throughout the life of the reactor.

The subassemblies were approximately 92 inches long, although the uranium fuel in the driver subassemblies was only about 14 inches long [7]. Above and beneath the fuel were neutron reflectors, which also began as depleted uranium but were later replaced with stainless steel. At the top of each subassembly was an adapter for removal, and at the bottom was an adapter which fit into a grid plenum support structure. Orifices at the bottom of each subassembly allowed sodium coolant to flow upward, with larger holes (and therefore greater flow) for those subassemblies in the

center region which produced the greatest heat [6]. The figures below show a cutaway of an EBR-II driver subassembly, revealing the components within [11].

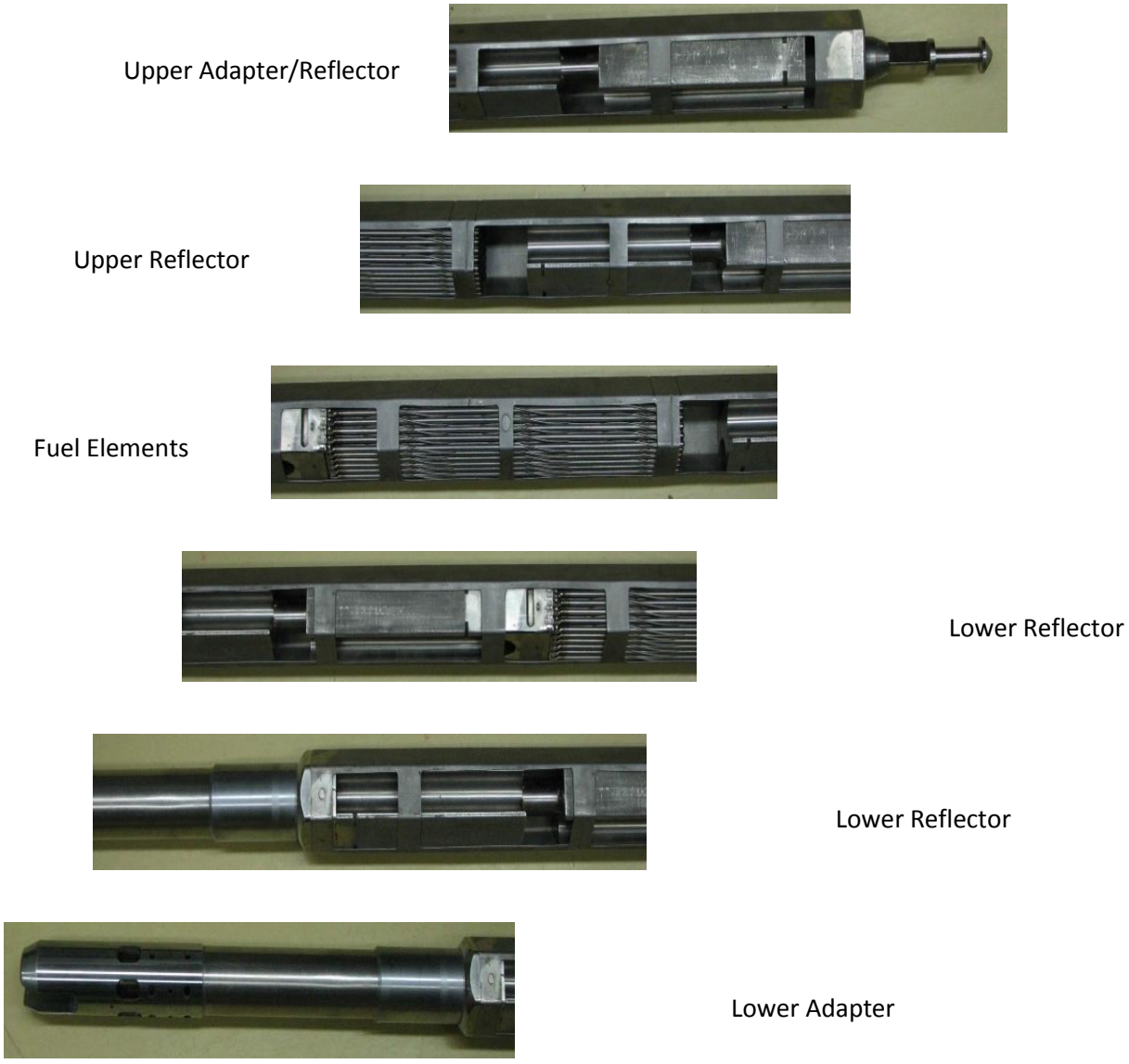

Figure 1: EBR-II driver assembly.

Figure 2: Fuel elements within an assembly.

The core was enclosed in a stainless steel reactor vessel. This vessel comprised of a radial shell, lower grid plenum structure, and upper reactor vessel cover which also served as a neutron shield. The top cover contained penetrations to allow for subassembly removal and the control rod drive mechanisms. Surrounding the reactor vessel radially were additional layers of graphite and borated graphite shielding. The entire vessel was submerged in about 10 feet of liquid sodium in a large pool-type design. The pool contained up to 89,000 gallons of sodium which was forced into the

core and blanket regions using two main centrifugal pumps [5] [6]. A diagram showing how these components fit together can be seen in Figure 3 [13].

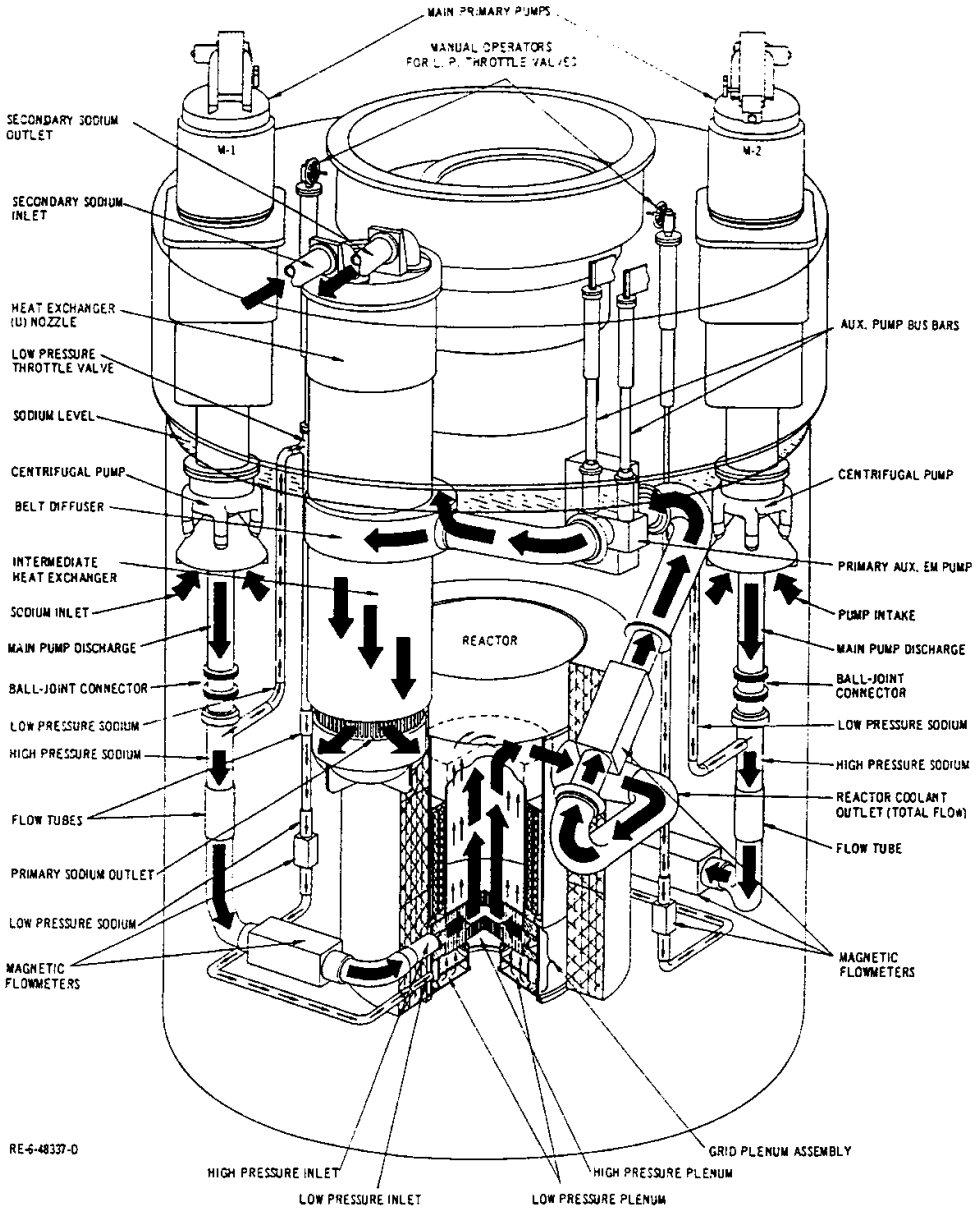

Figure 3: EBR-II primary system.

EBR-II was an extremely desirable candidate for a benchmark evaluation because of its unique capabilities. These capabilities were proven during a program called the

Integral Fast Reactor initiative, which lasted from 1984 through 1994. It was the goal of this program to solve many of the perceived problems of nuclear energy through scientific means. Problems that were addressed included safety, fuel reprocessing, waste, and proliferation [4]. The design of the EBR-II included many safety features. It was proven that the sodium coolant is extremely compatible with the stainless steel cladding and container, which prevents corrosion with the associated risk of radioactive release. The coolant was kept at near atmospheric pressure, thus insuring that any leak would ooze out in a slow and controllable manner. The metal fuel combined with metal cladding and metal coolant provided for an extremely high thermal conductivity, allowing heat to be easily removed from the reactor. The large volume of sodium in the pool, along with the large margins to sodium boiling meant that large amounts of heat could be absorbed by the system before incurring problems. Furthermore, at higher temperatures the reactor would thermally expand, resulting in increased neutron leakage from the core. This extra leakage caused a large negative temperature reactivity feedback which automatically shut the reactor down in case of an accident [4].

The safety features were put to the test in two landmark safety experiments conducted on EBR-II in April 1986. The tests simulated the loss of reactor coolant flow, as well as the loss of a heat sink. For each test the reactor was at 100% power, and in neither test was the reactor scrammed. In both cases the reactor shut itself down due to the physics of the design, and a safe steady state temperature was achieved through passive means [4]. Because of the importance of these tests, the particular reactor

configuration at the time of these tests was chosen as the configuration to be used in the reactor benchmark and sensitivity analysis.

The problems of fuel supply, waste, and proliferation were solved through the development of an innovative on-site reprocessing plant. This reprocessing plant was integral to the power plant, thus coining the name "integral fast reactor." Fuel coming from the reactor was chopped into pieces and placed into an electro-refiner within an anode basket. With the application of a voltage the desired elements such as uranium, plutonium, and minor actinides could be transported to a cathode. From there any impurities were boiled off in a cathode processor, and the resulting metal could be recast into new fuel using an injection casting furnace. Everything remaining in the electro-refiner, including the fission products with relatively short half-lives, could be disposed of in various waste forms [4]. This technology allowed for the potential to recycle most of the fuel back into the reactor, drastically reducing both the volume as well as the long term radioactivity of the waste. In fact, within approximately 300 years the waste (consisting mostly of fission products) would be less radioactive than the original uranium ore [4]. The only input required to sustain the reactor fuel cycle is uranium 238, which is inexpensive and in great abundance. It is also important to note that the electro-refiner was technically unable to separate plutonium in a pure form, rather it was always mixed with minor actinides and uranium [4]. This made the plutonium unsuitable for a weapon, and only able to handle using remote equipment from within a heavily shielded environment. This made the possibility of using anything acquired from this process for clandestine purposes very remote indeed.

It is important to recognize that these impressive capabilities were dependent on the features of the design discussed at the beginning of this chapter, namely pool-type, sodium cooled, metal fueled, and fast neutron spectrum. It is hoped that a benchmark of this important reactor will assist in the future development of similar reactors for commercial purposes.

Chapter 4: Sensitivity Analysis

As the goal of this project was to perform a sensitivity analysis on the EBR-II, it will be the purpose of this chapter to describe what a sensitivity analysis is, how it is done, and why it is important.

A sensitivity analysis is performed to determine how sensitive a dependent variable is on an independent one. In the case of the EBR-II, the goal of the analysis was to determine how sensitive the effective neutron multiplication factor (k-eff) is on the various neutron cross-sections for each isotope in the system. For example, if the fission cross section of U-235 is made larger, one would expect neutron production to increase and k-eff to go up. Conversely, if the capture cross section of U-235 is made larger, one would expect neutron loss to increase, and k-eff to go down. Another goal in performing the sensitivity analysis was to determine the effect that the density of certain mixtures has on k-eff. For example, if the fissile fuel mixture is made denser, one would expect k-eff to go up. Of course the results must be quantified in order for them to be useful.

The sensitivity analysis was performed through the use of the SCALE VI software package, specifically the KENO and TSUNAMI components of that package. The primary purpose of KENO is to allow the user to model a system and calculate k-eff. The purpose of TSUNAMI is to either create a model or import one that was made in KENO, and perform a sensitivity analysis on it. In order to understand how the sensitivity

analysis if performed, it is helpful to have a basic understanding of how KENO actually calculates k-eff.

KENO uses probabilistic (also known as Monte Carlo) methods to perform its calculations. It does this by creating neutrons and tracking them through the system. When a neutron is created, it will travel in a certain direction with a certain speed. The direction must be chosen at random, and this is done through the use of a random number generator. A random number is created between 0 and 1, and scaled to represent an angle between 0 to 2π for the horizontal direction. The vertical direction is chosen in a similar manner. The speed is chosen using a probability density function that represents the speed at which neutrons are born. Once a neutron is traveling, it must be randomly determined how far it will go before colliding with something, and this is done using the macroscopic total cross section (Σ_t) for that region. The distance a neutron will travel before a collision is given by:

$$X = -\ln(\zeta) / \Sigma_t \qquad \text{Eq. 1}$$

In the equation above, ζ is a random number between 0 and 1. During this process the neutron may leak from the system, and a new neutron will be created to replace it. It may also collide with nucleons, and in this case it is determined randomly which atom is collided with, based upon the atom density of the various atoms present. Whether the collision results in a scattering, capture, or fission event is determined according to the probability that each will happen, which is proportional to the size of the respective cross sections. If a neutron is scattered, a new energy and direction will be determined.

If a fission occurs, more neutrons will be created from that location and likewise tracked through the system. A diagram illustrating the various possibilities can be seen in Figure 4.

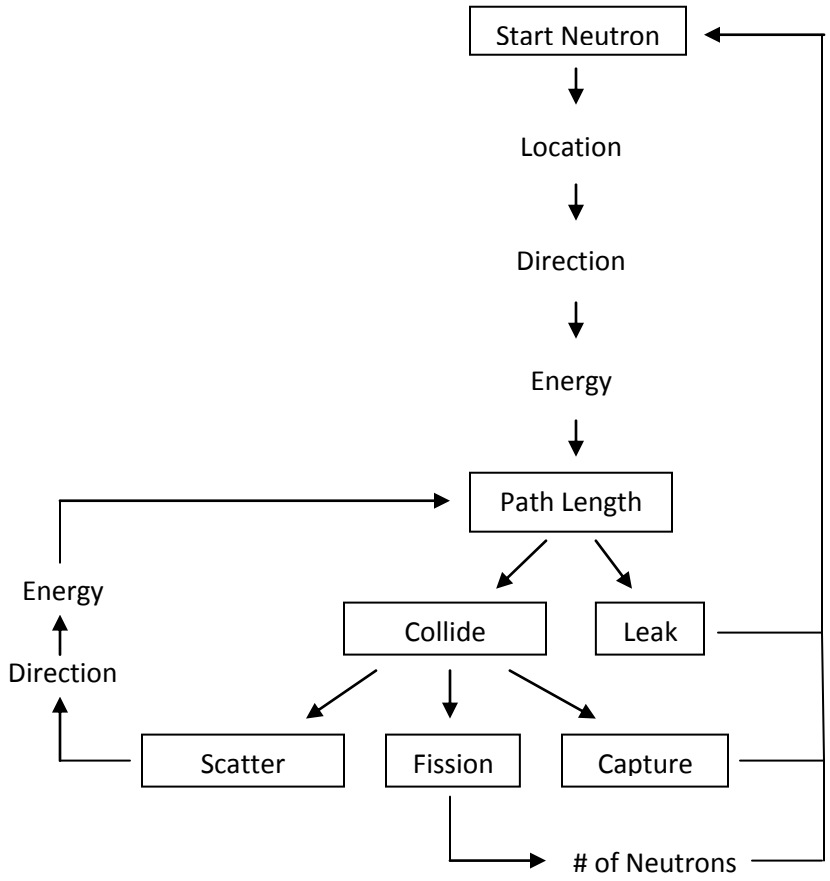

Figure 4: Neutron tracking diagram.

The ratio of neutrons created in the system through fission to the neutrons lost through leakage and absorption will determine the value for k-eff. If k-eff is greater than one, the neutron population would grow without bound. In order to limit the neutron population, k-eff is calculated in batches, with each batch called a generation. The user can specify the number of generations, as well as the number of neutrons to be tracked per generation, using the fission sites as starting locations. In order to get accurate

results with small statistical uncertainties, millions or even billions of neutrons must be tracked.

With an understanding of how k-eff is calculated, the first method of performing a sensitivity analysis can be discussed, which is called the direct perturbation method. A perturbation is a small change made to the system. The direct perturbation method means that a small change is actually made to the model, and k-eff calculated and compared to the nominal value. Usually a change is made in both directions, for example the density of a material might be increased and then subsequently decreased by 1% from the nominal value. The sensitivity coefficient can be calculated by the following equation [3]:

$$S_{k,\alpha} = \frac{\alpha}{k} \times \frac{dk}{d\alpha} = \frac{\alpha}{k} \times \frac{k_{\alpha^+} - k_{\alpha^-}}{\alpha^+ - \alpha^-} \qquad \text{Eq. 2}$$

Where α is the nominal value for whatever is being perturbed, α^+ and α^- are the upper and lower values respectively, k is the nominal value for k-eff, and k_{α^+} and k_{α^-} are the upper and lower values respectively. The standard deviation for the sensitivity coefficient can be calculated with the following equation [3]:

$$\sigma_S = \left(\left(\frac{\left(\sigma_{k^+}^2 + \sigma_{k^-}^2\right)}{\left(k^+ - k^-\right)^2} + \frac{\sigma_k^2}{k^2} \right) \times \left(\frac{k^+ - k^-}{k} \right)^2 \right)^{1/2} \times \frac{\alpha}{\alpha^+ - \alpha^-} \qquad \text{Eq. 3}$$

where all values present in equation 2 have the same meaning in equation 3, σ_k is the standard deviation for the nominal calculation of k-eff, and σ_k^+ and σ_k^- are the standard deviations for the upper and lower k-eff calculations. It is clear that with millions or even billions of particle tracks being performed for every k calculation, it would be extremely time consuming to use the direct perturbation method for more than a small amount of perturbations. To save time, first order perturbation theory is used, as described below.

Rather than repeating the original criticality calculation again and again for every change made to the system, perturbation theory allows one to mathematically solve for the new value of k, assuming the perturbation is sufficiently small. It may be remembered from reactor physics classes that the steady state neutron diffusion equation can be written as:

$$-\nabla D \nabla \Phi + \Sigma_a \Phi(\mathbf{r}) = (1/k)\nu\Sigma_f \Phi(\mathbf{r}) \qquad \text{Eq. 4}$$

With a simplified form of the equation being:

$$M\Phi = (1/k)F\Phi \qquad \text{Eq. 5}$$

Where M is the destruction operator (absorption plus leakage), F is the production operator (fission), and Φ is the neutron flux [10]. In multigroup diffusion M, F, and Φ are matrices that represent the values for the different neutron energy groups. Furthermore it must be understood that the definition of an inner product (f,g) between two functions f(r) and g(r) is:

$$(f,g) = \int_v d^3r\, f^*(r)g(r) \qquad \text{Eq. 6}$$

Where f*(r) represents the complex conjugate of f(r) and $_v$ is the core volume [10]. The operator M† which is adjoint to the operator M can now be defined using inner products as:

$$(M^\dagger f,g) = (f,Mg) \qquad \text{Eq. 7}$$

If reactivity is defined as:

$$\rho = (k-1) / k \qquad \text{Eq. 8}$$

then perturbation theory allows us to calculate the change in reactivity with the equation:

$$\Delta\rho = (\Phi^\dagger,[\delta F - \delta M]\Phi) / (\Phi^\dagger, F\Phi) = 1/k - 1/k' \qquad \text{Eq. 9}$$

Where $\Phi^\dagger$ is the adjoint flux, δF and δM are the changes to the destruction and production operators, and k' is the perturbed value of k [10]. As can be seen from equation 9, if the nominal value for k is known along with the flux, adjoint flux, and material properties, then the value for k' can be solved for mathematically without having to redo the entire calculation. In the process of solving the equation a series is formed. Because the second and higher order quantities in the equation have a much smaller effect on the outcome than the first quantity, these are usually discarded, and the answer becomes a first order approximation, hence the name first order perturbation theory [10].

A simple example helps to illustrate the value of perturbation theory [10]. Consider a reactor in the form of a bare (unreflected) slab, the width of which is characterized by the letter "a." The reactor will be analyzed using one-speed diffusion theory, which has the advantage of causing the flux and the adjoint flux to be self-adjoint, which means that they are equal to one another. The unperturbed flux in the reactor is:

$$\Phi(\mathrm{x}) = \Phi(0)\sin\left(\frac{\pi \mathrm{x}}{\mathrm{a}}\right) \qquad \text{Eq. 10}$$

where $\Phi_{(0)}$ is the flux in the center of the slab. Now consider an additional neutron absorber is homogeneously added to the slab from 0 to h, where 0 represents the left edge of the slab and the variable "h" represents some distance into the slab. First order perturbation theory allows one to calculate the change in reactivity due to the additional absorber as:

$$\Delta\rho = -\frac{\int_0^a \delta\Sigma a \phi^2 dx}{\nu\Sigma f \int_0^a \phi^2 dx} = -\frac{2}{\pi}\frac{\delta\Sigma a}{\nu\Sigma f}\left[\frac{\pi h}{2a} - \frac{1}{4} sin\frac{2\pi h}{a}\right] \qquad \text{Eq. 11}$$

In equation 11, $\delta\Sigma_a$ is the change to the macroscopic absorption cross section in the perturbed area. With this known, calculating the change in reactivity becomes a simple matter, and can be done rapidly for many cases. This is far more convenient than solving the diffusion equation every time a change is made.

When a sensitivity analysis is performed in TSUNAMI, the software begins by running KENO to solve for the flux, as well as the nominal value of k. It then runs a new calculation to solve for the adjoint flux [3]. More information about the adjoint flux and

how it is calculated can be found in Appendix B. With this information, the computer code can mathematically and very rapidly perturb the various cross sections of each isotope present in the system to determine the effect it has on k-eff. It can also rapidly perturb the density of each mixture present. The final results are then displayed for the user. Before the displayed results can be trusted however, it is very strongly recommended that the user perform at least one sensitivity analysis using the direct perturbation method, and compare the sensitivity coefficient from equation 2 with the sensitivity coefficient generated by first order perturbation theory [3].

A sensitivity analysis contributes to a benchmark by quantifying how strongly uncertainties in isotopic cross sections and material densities effects the calculated multiplication factor of the reactor. If therefore the calculation results for an experiment do not match the benchmark values, a sensitivity analysis can help determine whether uncertainties in the material data might be the issue or not.

Chapter 5: KENO VI Core Model

Before a sensitivity analysis could be performed on the EBR-II, it was necessary to create a detailed computer model of the reactor core. Before this could happen, a great deal of information was needed such as geometry and material specifications. Geometry specifications included things like fuel slug diameter and length, cladding thickness, and lattice spacing. Material specifications including things like fuel, coolant, and cladding compositions. Over a period of several weeks a great deal of information was gathered from a variety of sources. These sources included engineering drawings for the various EBR-II subassemblies, reports from Argonne National Laboratory [6] [7], books published on the EBR-II [4] [5], and other documents [11] [12]. With these sources available, work was begun sifting through the available data to extract those things that would be useful in creating a detailed reactor model.

The model was created using the KENO component of the SCALE software package, released by Oak Ridge National Laboratory. The first step was to define the various material compositions that would be used in the model. These included the uranium fuel mixture for the fuel rods, depleted uranium for the blanket rods, sodium for the coolant, and stainless steel types 304 and 316 for the cladding and hexagonal ducts [7]. For each material the weight percent of each nuclide present had to be specified, as well as the overall material density. The depleted uranium, sodium, and stainless steel were all created as “clean” mixtures, meaning that the buildup of minor isotopes due to the neutron flux for these regions were not included in the model. The

uranium fuel mixture was also initially modeled as fresh fuel, without taking any burnup into account. Defining the main core materials individually however was not enough, there were other parts of the reactor core above and below the fueled section that were modeled as a homogeneous mixture, rather than modeling the actual internal shapes. This was done because the relative neutron flux in these areas is small compared to the core region and therefore comparatively unimportant. It also helped save calculation time, and simplified the regions that were fairly complex. Care was taken to estimate the volume percent that each material occupied, and these mixtures were also defined. Sections that were to be modeled homogeneously included the upper and lower shields, reflectors, and adapters, as well as the empty portion of the fuel rods above the fuel slugs, and the B_4C poison region above the control rods [7]. The depleted uranium outer blanket and stainless steel inner blanket were also initially modeled as homogenous mixtures.

With the individual materials defined, as well as the various homogenous mixtures, work was begun to model a single fuel element. This initially consisted of a fuel slug, surrounded by sodium, surrounded by cladding, all surrounded by more sodium [7]. Each fuel element had a wire that wrapped around it from the top to the bottom to provide for spacing, and this was modeled with a straight wire that ran the length of the fuel element. A 3D picture of this original fuel element can be seen in Figure 5.

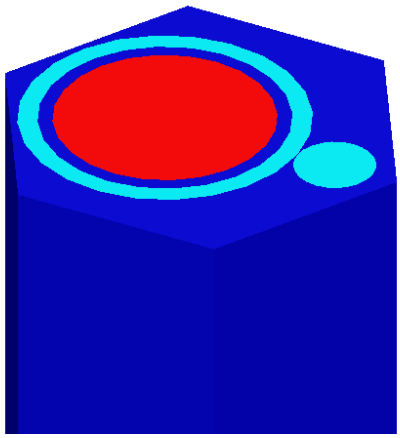

Figure 5: Fuel element.

The red color represents the uranium fuel, the light blue represents stainless steel 316, and the dark blue represents the surrounding sodium. To show how each portion extends, a cutaway view can be seen in Figure 6.

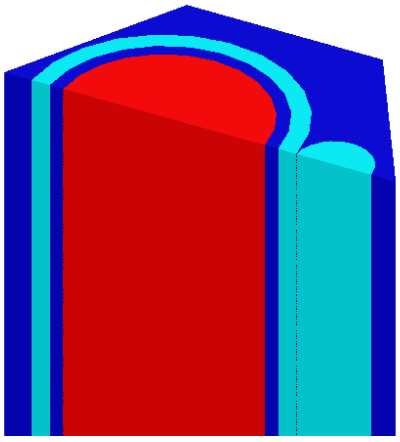

Figure 6: Fuel element cutaway view.

After creating one fuel element, this was then placed within an array to create a hexagonal lattice of 91 fuel elements. These were surrounded by a stainless steel

hexagonal duct, which was also surrounded by sodium. This represented the fueled section of the driver subassembly [7]. A cross section view can be seen in Figure 7.

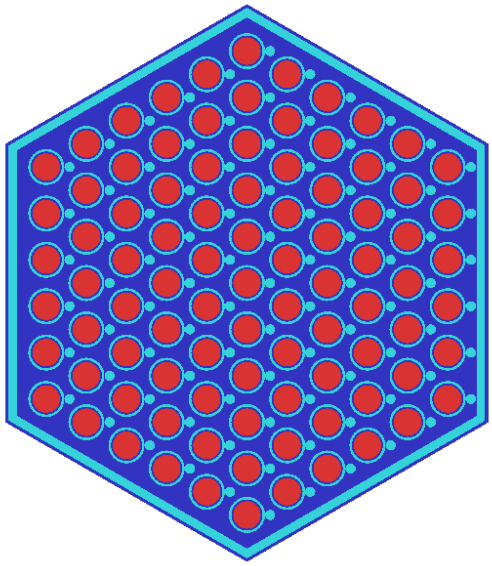

Figure 7: Driver subassembly cross section.

After creating this section, the other portions had to be added. These included the upper and lower adapters and shields (reflectors), as well as the gas plenum within the fuel elements. Putting them all together completed the entire driver subassembly, as seen in Figure 8.

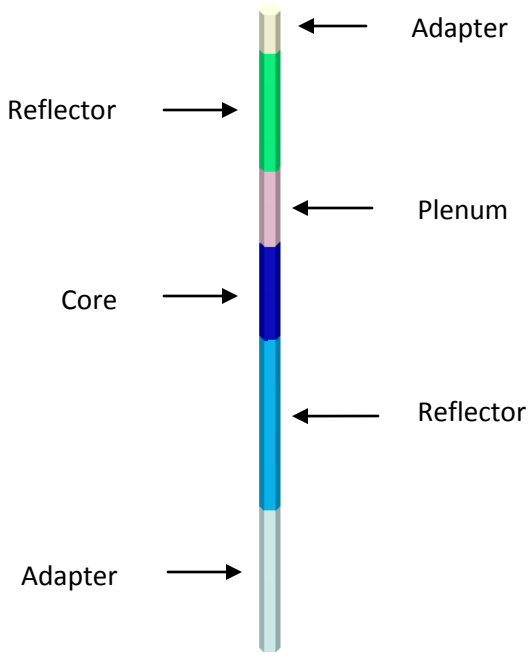

Figure 8: Driver subassembly.

In Figure 8 above the active fuel region is the dark blue section in the middle. This shows how small it was compared to the subassembly as a whole. Some of the driver subassemblies only contained half the number of fueled elements, with the others being replaced by stainless steel [7]. These were known as half-worth driver subassemblies, and can be seen in Figure 9.

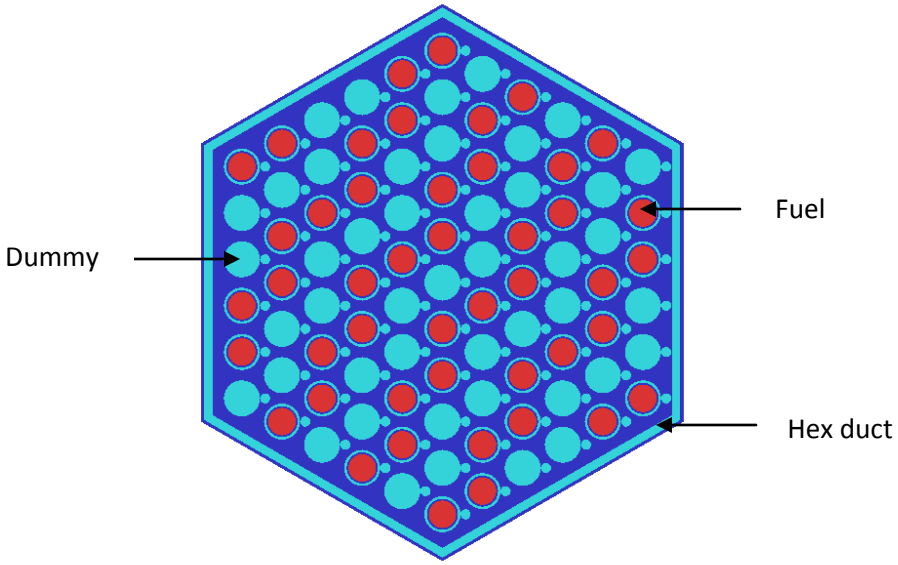

Figure 9: Half-worth driver subassembly.

The reactor was controlled by inserting two safety subassemblies into the core simultaneously, followed by the insertion of control subassemblies one by one until criticality was reached [6]. The major difference between the two was that the control subassemblies included a B_4C poison region above the fuel to maximize the reactivity swing when they were withdrawn. Both types of subassemblies contained 61 fuel elements [7]. These were surrounded by an inner and an outer stainless steel hex duct and sodium, as seen in Figure 10.

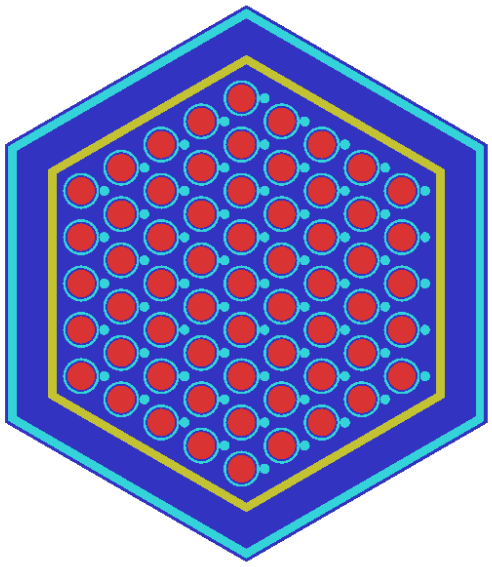

Figure 10: Safety/control subassemblies.

The inner hex duct was understood to be made from stainless steel 304, as represented by the yellow color.

Also in the core were several dummy subassemblies, which consisted of 7 large stainless steel rods within a hex duct surrounded by sodium [7]. This can be seen in Figure 11.

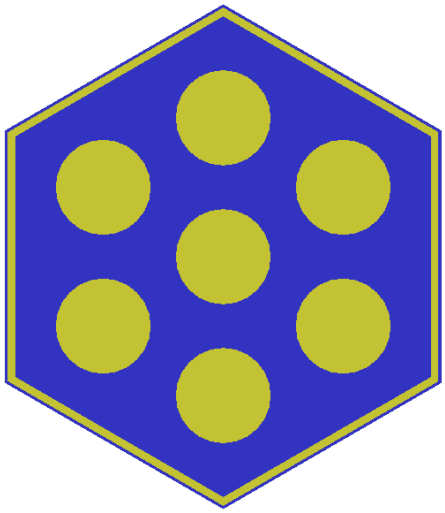

Figure 11: Dummy subassembly.

The last category of subassemblies within the core were experimental/instrumentation subassemblies, all of which differed from one another. Although the specifics of these subassemblies were not fully clear, they were modeled as best understood from the available documentation. Three of these were the XX09, XX10, and XY-16 subassemblies. The XX09 was modeled the same as a safety subassembly, except with two of the fuel rods being replaced by stainless steel. The XX10 was modeled as 19 stainless steel rods within two hex ducts. The XY-16 was also modeled the same as a safety subassembly, except that all of the fuel elements were replaced by stainless steel [7]. These can be seen in Figures 12, 13, and 14 respectively.

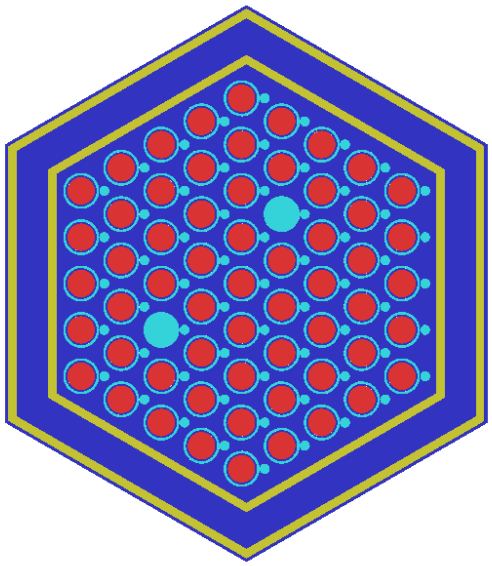

Figure 12: XX09 subassembly.

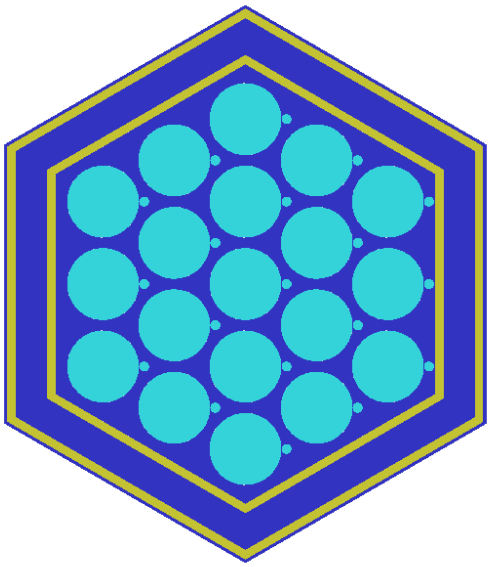

Figure 13: XX10 subassembly.

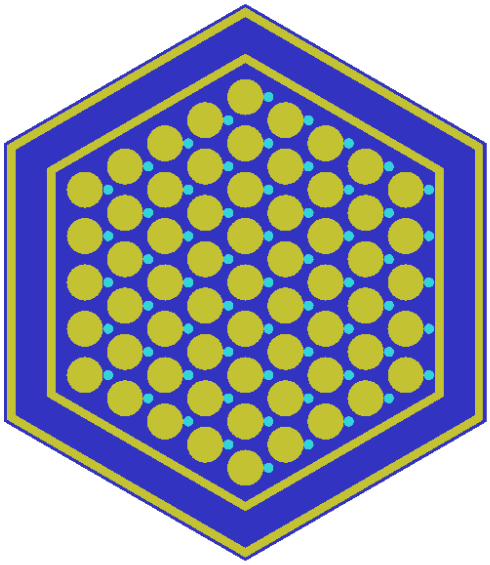

Figure 14: XY-16 subassembly.

The inner blanket which surrounded the core was composed of stainless steel reflector subassemblies, which consisted of a hexagonally shaped chunk of steel surrounded by a hex duct, as seen in Figure 15. The outer blanket which surrounded the inner blanket was composed of subassemblies containing 19 depleted uranium rods surrounded by sodium, held within stainless steel cladding, all surrounded by a stainless steel hex duct, as seen in Figure 16 [7].

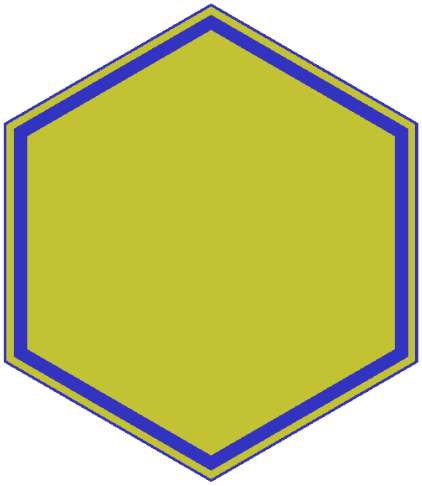

Figure 15: Reflector subassembly.

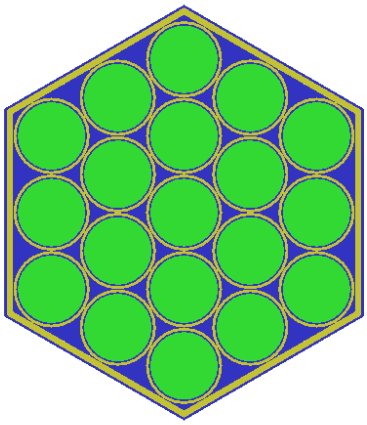

Figure 16: Depleted uranium subassembly

When all of the necessary subassemblies were created, they were placed in an array to match the configuration of the core at the time of the landmark heat removal tests mentioned in Chapter 3 [7]. At first the inner and outer blanket regions were

modeled as homogeneous mixtures. A cross section view of the model can be seen in Figure 17.

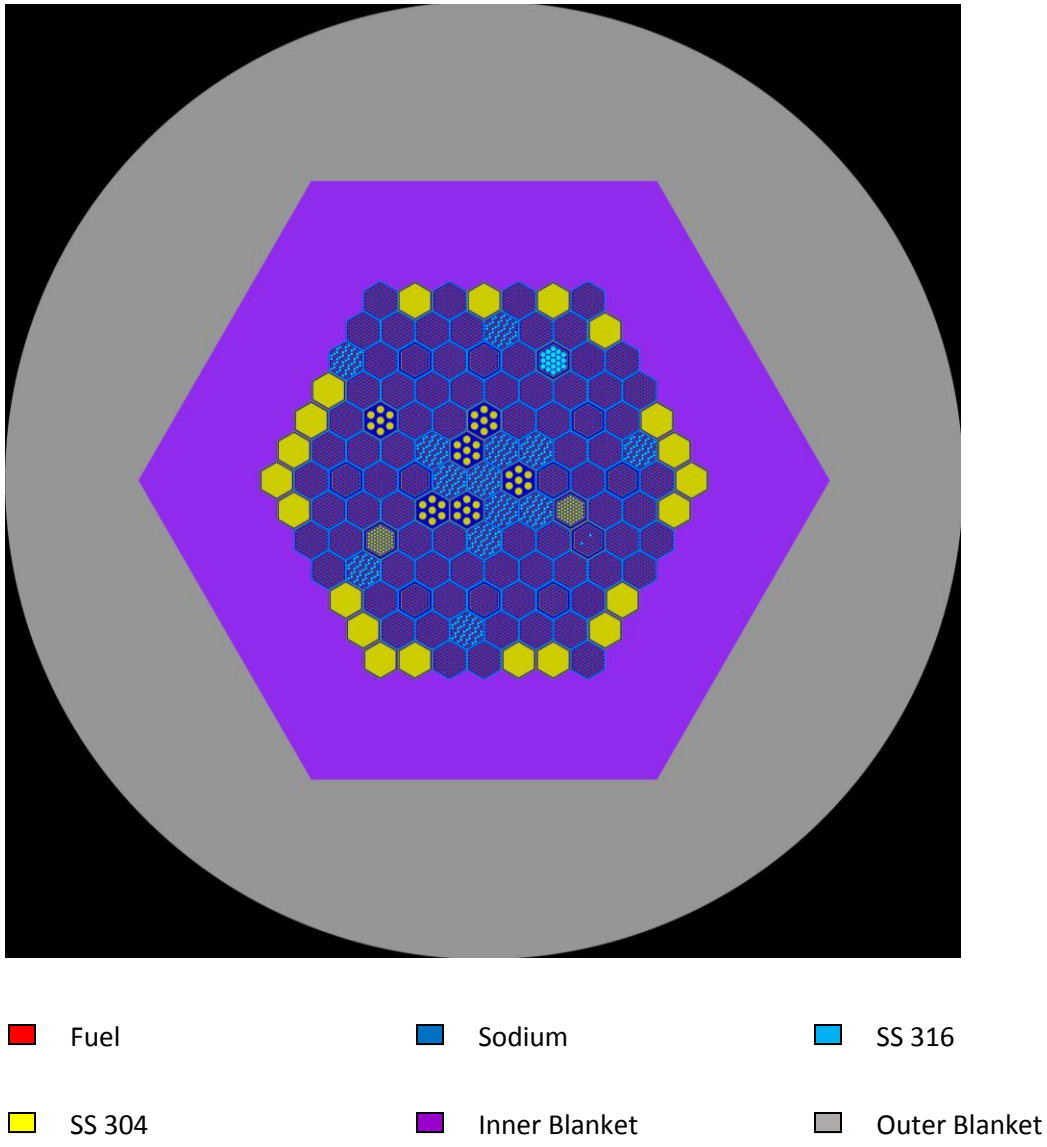

Figure 17: Initial core model.

The black region represents void, as nothing outside the outer blanket was modeled.

With the entire core modeled, a criticality calculation was performed to determine the value for k-eff. This could then be compared with expected values to see

if the model approached reality. With all of the safety and control subassemblies fully inserted the value for k-eff came out to be 1.1094 ± 0.0018. This result was higher than expected, and was confirmed to be too high when all of the control subassemblies were completely removed yielding a k-eff of 1.0778 ± 0.0015. With the control rods removed k-eff should have been below 1.0, so it was clear that some more adjustment was needed.

More research was done to determine what should be adjusted in the model, and several actions were taken. First the sodium density was lowered to account for the temperature within the reactor, which was modeled at 650 F to represent the temperature at the time of going critical (the operational temperature was around 700 F going into the reactor, and around 880 F coming out) [5]. The neutron cross section data was likewise adjusted for temperature. Of greater importance was the fact that the driver subassemblies in the EBR-II did not contain fresh fuel as had been modeled, but rather each subassembly had a unique burnup level and composition [7]. The composition data for each driver subassembly was organized and averaged together. This average composition was then set as the fuel mixture. It was also known that the metal fuel slugs in the EBR-II became swollen after a few percent burnup, to the point that they came into contact with the surrounding cladding [11]. The combined radial and axial swelling decreased the fuel density [12]. The model was adjusted to account for this phenomenon, which turned out to have a significant influence on k-eff. Finally it was decided to change the inner and outer blanket so that they were no longer a homogeneous mixture, but rather were modeled according to their actual geometry. It

turns out that the homogenous assumption for those regions had very little impact on k-eff, but it was important to find out, and the change made for a much better looking model. The final result can be seen in Figure 18.

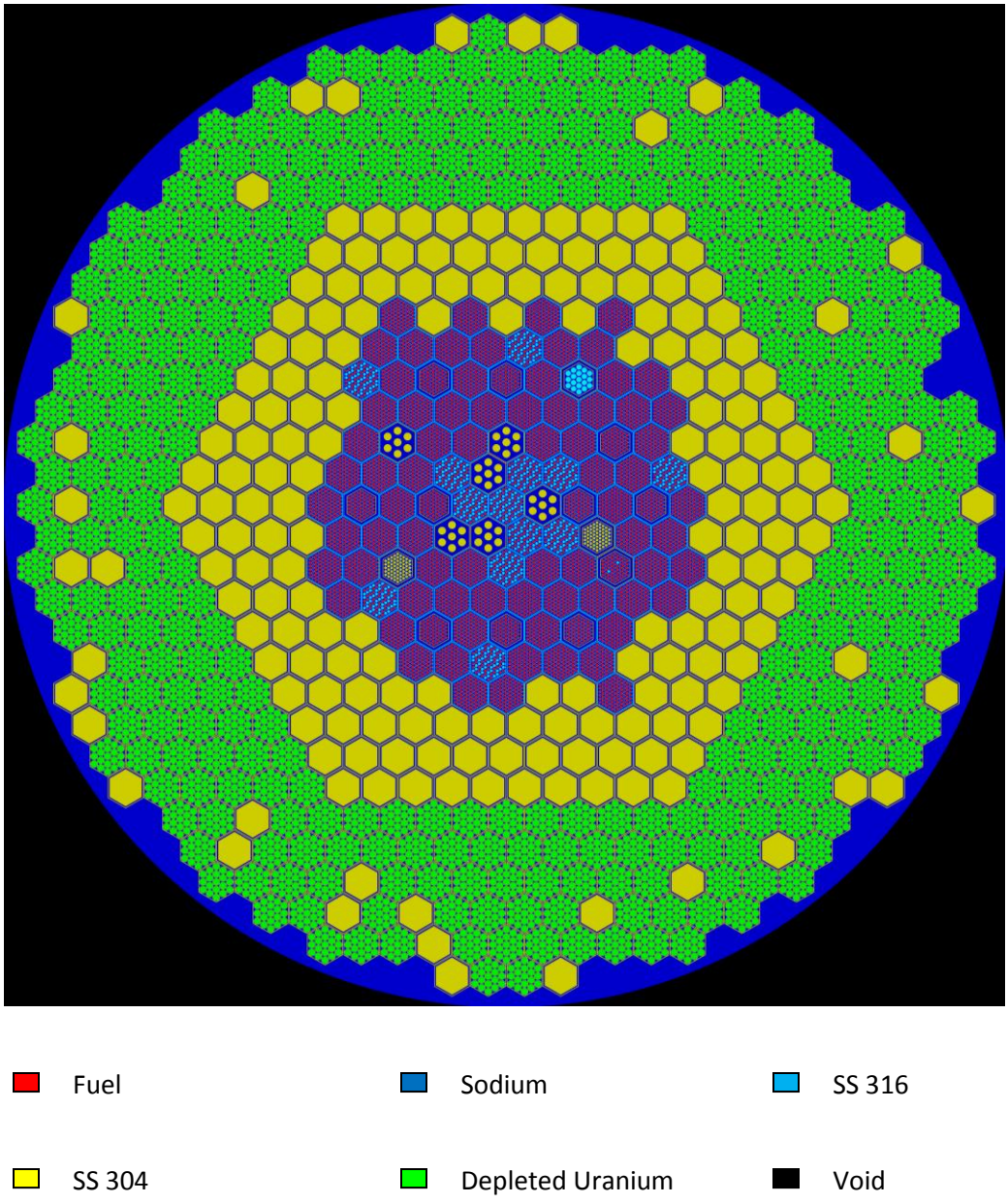

Figure 18: Final core model.

To create such a detailed model that is based on accurate reactor data took an enormous amount of time and effort. The complexity of the model can be appreciated by examining the input file, which can be found in Appendix C. Some of the key parameters of the KENO reactor model can be seen in Table 1.

Table 1: KENO Model Key Parameters

Total assemblies	637
Driver	73
Half-worth driver	13
Outer blanket	330
Stainless steel reflector	201
Control rods	8
Safety rods	2
Stainless steel dummy	6
Experiments	2
Instrumented	2
Hex duct internal flat to flat (cm)	5.6134
Hex duct thickness (cm)	0.1016
Lattice spacing (hex duct pitch) (cm)	5.8929
Fuel cladding thickness (cm)	0.0248
Fuel slug diameter (cm)	0.3924
Fuel slug length (cm)	36.65
Fuel density (g/cm^3)	12.43
Lattice spacing (fuel rod pitch) (cm)	0.5660
U-235 (g) / driver assembly	3045
U-238 (g) / driver assembly	1603
Fuel Alloy Composition (wt %)	
U-235	60.72
U-238	31.97
Molybdenum	3.14
Ruthenium	2.50
U-236	0.61
Rhodium	0.36
Palladium	0.24
Pu-239	0.16
Zirconium	0.13
La-139	0.12
Nd-148	0.03
Niobium	0.01
Other	0.01

With the changes made to the model as described above, a new criticality calculation was performed. With safety and control rods completely inserted, k-eff was calculated to be 1.05085 ± 0.00054. Two of the eight control subassemblies were then lowered around 14 inches, with another one lowered around 11 inches. These represented the control rod positions at which the EBR-II went critical. K-eff was then calculated to be 1.03873 ± 0.00088. Although still too high, this was much closer to the expected value than the previous configuration had been. Rather than continue to make adjustments, the model was deemed to be of sufficient quality to perform a sensitivity analysis on the EBR-II. This is because a sensitivity analysis does not depend so much on the absolute value of k-eff, as it does the change in k-eff due to a perturbation.

With the KENO model finished it was time to execute TSUNAMI for the sensitivity analysis. A cross-section data library containing 238 energy groups was chosen. At this point the model could either be analyzed as a homogeneous mixture, or the lattice geometry of the fuel could be specified to account for resonance self-shielding effects [3]. Both were compared and found to give similar results, likely because the neutrons remain in the fast spectrum rather than slowing down to resonance energies. Nevertheless the latter was used as this was recommended for the greatest accuracy. For the final run, the flux was calculated using 250 generations of 10,000 neutrons each (with 50 generations being skipped), and the adjoint flux was calculated using 1,000 generations of 1,000,000 neutrons each (200 skipped). The skipped generations allow the neutron flux shape to change from the source definition

to the fundamental mode before beginning averaging calculations, which helps reduce error.

The sensitivity analysis was performed at maximum reactivity, that is, with all control rods fully inserted. It was desired however to find out if the results would be different when the control rods were adjusted to represent the EBR-II critical rod heights, because this would introduce more boron into the core. The adjustment was made and a new sensitivity analysis performed.

One shortcoming of the model that had been created was that the fuel composition did not include certain fission products, due to them being lumped together in the subassembly composition data. It was therefore necessary to perform a depletion analysis, which when coupled with a sensitivity analysis, would determine their importance. Within the SCALE package is a software sequence known as TRITON. This has the ability to take a model, calculate the flux, and determine the isotopic composition for a specific level of burnup. To use this feature, a homogeneous sphere of U-235, U-238, sodium, and a small percentage of other elements was modeled. The weight percent of each isotope represented fresh EBR-II fuel. EBR-II fuel was able to handle much higher burnup levels than current light water reactor fuel, with values ranging from 80,000 to 150,000 MWd/MTHM [12]. 80,000 MWd/MTHM was chosen for use with the sensitivity analysis. The resulting isotopic composition was compared with the top 25 nuclides from another depletion analysis that had been performed on an EBR-II subassembly, and was found to be similar [12]. The weight percent for each isotope present was then calculated, and those that had a weight percent of 0.000001%

or higher were included in the new fuel composition. A new sensitivity analysis was then performed using the same parameters as before.

Chapter 6: Analysis Results

Results from the sensitivity analysis can be displayed in various ways. Usually the result most desired is to know which nuclide cross sections have the greatest effect on k-eff, when the perturbation effects are integrated over all neutron energies, reactor regions, and material mixtures. The result for the top 15 nuclides can be seen in Table 2, with an extended list available in Appendix A.

Table 2: Integrated Nuclide Sensitivity Coefficients

Nuclide	Reaction	Sensitivity	Std. Dev.	% Std. Dev.
^{235}U	nubar	9.6081E-01	1.12E-04	0.01%
^{235}U	fission	5.2769E-01	4.91E-04	0.09%
^{235}U	total	4.5810E-01	1.07E-03	0.23%
^{235}U	n,gamma	-9.2460E-02	1.06E-04	0.11%
^{235}U	capture	-9.2460E-02	1.06E-04	0.11%
^{56}Fe	scatter	5.7375E-02	8.36E-04	1.46%
^{56}Fe	elastic	5.1578E-02	8.03E-04	1.56%
^{56}Fe	total	4.6199E-02	8.39E-04	1.82%
^{23}Na	scatter	3.8391E-02	9.63E-04	2.51%
^{23}Na	total	3.7402E-02	9.63E-04	2.57%
^{23}Na	elastic	3.4656E-02	9.31E-04	2.69%
^{238}U	nubar	3.4056E-02	8.68E-06	0.03%
^{238}U	capture	-2.8369E-02	2.98E-05	0.10%
^{238}U	n,gamma	-2.8369E-02	2.98E-05	0.10%
^{235}U	scatter	2.2863E-02	5.62E-04	2.46%

In Table 2 the left two columns specify the cross section type, and the third column specifies the sensitivity coefficient. This is the percent change in k-eff due to a 1% increase of the specified cross section for all energies [3]. For example, a 1% increase in

the U-235 fission cross section leads to a 0.52769% increase in the value of k-eff. A 1% increase in the U-235 capture cross section on the other hand corresponds to a 0.09246% decrease in k-eff. The fourth and fifth column specify the standard deviation and standard deviation % of the sensitivity coefficient.

To grasp the relative magnitude of the data found in Table 2, it is helpful to see the results displayed in graphical form. Figure 19 shows the sensitivity of k-eff to the first five nuclide reactions of Table 2 at the various neutron energies. Figure 20 shows the next seven nuclide reaction sensitivities plotted against that of U-235 nubar($\overline{\nu}$). This was chosen as a reference because it has the largest sensitivity coefficient. Nubar, rather than being a cross section in the traditional sense, represents the number of neutrons released per fission for a given incident neutron energy.

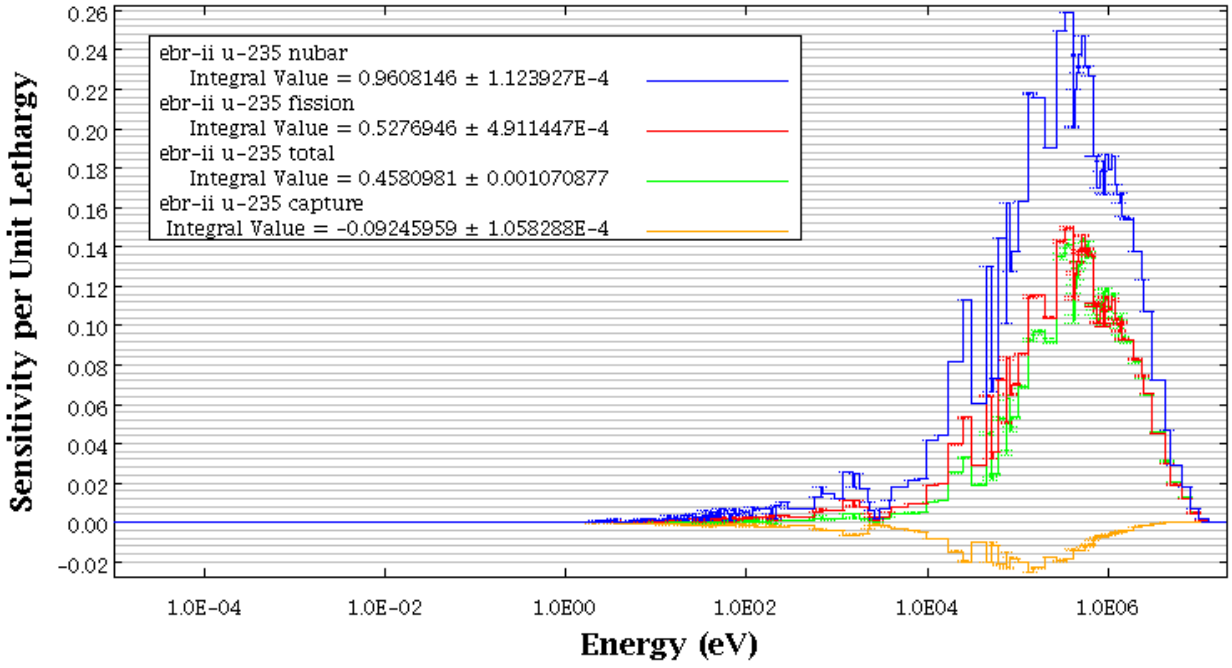

Figure 19: Sensitivity plot 1

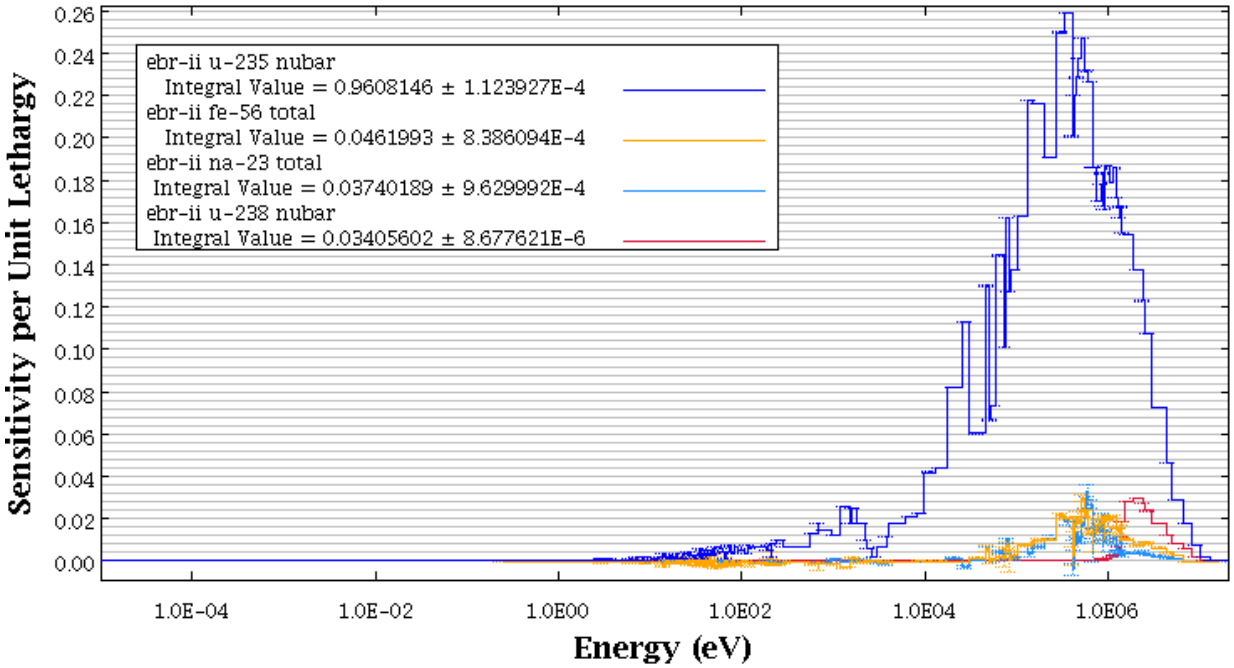

Figure 20: Sensitivity plot 2

It is clear that k-eff is only sensitive to perturbations in cross sections at high neutron energies. This is to be expected, as there are very few thermal neutrons in the core.

When a neutron is absorbed by a nucleus without causing fission, the event is known as neutron capture. The capture of a neutron can result in several outcomes such as the release of a proton, alpha particle, or other neutrons. For U-235 the most likely outcome of neutron capture is the release of a gamma ray, causing the capture and n,gamma cross sections to be nearly identical. For this reason the U-235 (n,gamma) cross section is not shown in the plot above. The sensitivities of the scatter and elastic cross sections for Fe-56 and Na-23 were also omitted from the plot because they were so similar to the total cross section.

The results from the depletion model showed that the reactor was extremely insensitive to any fission product cross sections. The analysis for the critical control rod configuration however confirmed that the sensitivity of k-eff to several boron cross sections was substantially increased in this case, while little else was affected. The results can be seen in Table 3. Even with the increased sensitivity however, boron still ranks fairly low when compared with other nuclides.

Table 3: Boron Sensitivity Coefficients

Nuclide	Reaction	Sensitivity	Std. Dev.	% Std. Dev.
^{10}B	capture	-5.5752E-03	1.82E-05	0.33%
^{10}B	n,alpha	-5.5483E-03	1.81E-05	0.33%
^{10}B	total	-5.5218E-03	4.04E-05	0.73%

Another result of great interest is to know the sensitivity of k-eff to the density of each mixture present in the reactor. The top 6 can be seen in Table 4, with the complete list in Appendix A.

Table 4: Mixture Sensitivity Coefficients

Mixture	Mixture Name	Sensitivity	Std. Dev.	% Std. Dev.
6	Fuel	4.6387E-01	1.15E-03	0.25%
5	SS 304	4.5698E-02	6.91E-04	1.51%
2	Sodium	2.4314E-02	8.69E-04	3.57%
9	Empty Fuel Rods	2.3490E-02	4.12E-04	1.75%
3	SS 316	1.9099E-02	4.87E-04	2.55%
10	Lower Driver Shield	1.1366E-02	3.95E-04	3.47%

The sensitivity coefficient provided in the third column represents the percent change in k-eff that results from a 1% increase in that mixture's density [3].

In order to validate the results of the sensitivity analysis performed by Tsunami, the results were compared with those from a direct perturbation (as described in chapter 4). This was only done for the model with depletion data. A direct perturbation was performed for the U-235 total cross section and fuel mixture density using equations 2 and 3. The results can be seen in Table 5 below.

Table 5: Direct Perturbation Comparison

Perturbation	Tsunami Results	Tsunami Std. Dev.	Direct Results	Direct Std. Dev.
U-235 Total (Σ_t)	5.0265E-01	7.45E-04	5.5901E-01	3.87E-02
Fuel Density	5.2483E-01	9.91E-04	5.4702E-01	3.92E-02

Although it is very useful to see the sensitivity of k-eff to different cross sections and mixtures, TSUNAMI takes this one step further and reports the uncertainty of k-eff due to the uncertainties tabulated in its own cross section covariance data. The covariance data describes not only the uncertainty of a particular nuclide reaction, but also the shared uncertainty between two different nuclide reactions, or between a nuclide reaction and itself at different energy levels [3]. The overall standard deviation of k-eff due to the uncertainties in cross section data was reported to be 2.2119 ± 0.0014 (% Δk/k). A list of the top 7 nuclide reactions and their contributions to this overall uncertainty can be seen in Table 6, with an extended list available in Appendix A.

Table 6: Uncertainty Information

Nuclide Reaction	Nuclide Reaction	Uncertainty Contribution
^{235}U n,gamma	^{235}U n,gamma	2.1777E+00 ± 1.3730E-03
^{235}U fission	^{235}U fission	2.1155E-01 ± 9.2017E-06
^{235}U elastic	^{235}U n,gamma	1.5587E-01 ± 1.0099E-04
^{235}U nubar	^{235}U nubar	1.4088E-01 ± 5.1463E-07
^{56}Fe elastic	^{56}Fe elastic	1.2223E-01 ± 4.4904E-05
^{235}U n,n'	^{235}U n,n'	1.2156E-01 ± 1.3147E-04
^{23}Na elastic	^{23}Na elastic	1.0730E-01 ± 8.8504E-05

Chapter 7: Conclusions

Upon studying the results, it is clear that k-eff for the EBR-II is by far most sensitive to the value of U-235 nubar, or in other words, the number of neutrons released per fission. A 1% increase in this value can increase the value of k-eff by almost 1%. That is extremely significant, when one considers an actual value for k of 1.000 would be reported as nearly 1.0096 due to this 1% difference alone. In order to have confidence in the calculated value of k, it is paramount that this information in the cross section data library is accurate. The U-235 fission and total cross sections are the next most important. While the sensitivity of k-eff to these cross sections is only approximately half that of nubar, a 1% error can still have a very significant effect on its value. Furthermore, a 1% error in any of these cross sections is very small, what if the data is off by 5%? This would have huge implications in the resulting calculations.

Starting with the U-235 capture cross section the sensitivity of k-eff drops by about an order of magnitude. Other cross sections in this range include Fe-56 scatter, Na-23 scatter, and U-238 nubar. If it is certain that the most important cross sections are already extremely accurate, then improving the accuracy of these cross sections would help improve the k calculation, especially if one of them is very far off.

If the covariance data within the SCALE library is an accurate representation of the actual uncertainties in the data, then by far the most important cross section to improve would be the U-235 (n,gamma) cross section. Although the sensitivity of k-eff to this cross section was only -0.09246% for a 1% increase, this cross section uncertainty

alone is causing a total k-eff uncertainty of 2.1777%. This is over 98% of the total uncertainty.

It should be mentioned here that for the EBR-II it is not necessary to improve the cross section data at all neutron energy levels. As seen in Figures 19 and 20, improving the data between 1.0E4 and 1.0E7 eV would be sufficient. For some of the nuclide reactions an even smaller range would suffice. U-238 nubar for instance is only applicable between 1.0E6 and 1.0E7 eV, as these high energies are required for U-238 fission to occur.

As far as the different material densities are concerned, the fuel mixture is easily the most important to k-eff, by more than a factor of 10. Small changes in fuel density have big implications on the criticality calculation. It is very important that this value be correctly determined if a computer code is to match a benchmark value. If this value is known, then improving the stainless steel and sodium densities can make a difference, as can the densities for the homogeneously modeled regions just above and below the fuel.

As seen in Table 5, the direct perturbation sensitivity results for the U-235 total cross section and fuel density were very similar to the calculated values using TSUNAMI. This builds confidence that the calculation results are accurate and can be trusted.

REFERENCES

[1] United States Environmental Protection Agency, “Clean Energy,” 2014, http://www.epa.gov/cleanenergy/energy-and-you/

[2] Nuclear Energy Agency, Organization for Economic Cooperation and Development, “International Handbook of Evaluated Reactor Physics Benchmark Experiments,” 2014

[3] Oak Ridge National Laboratory, “TSUNAMI Primer: A Primer for Sensitivity/Uncertainty Calculations with SCALE,” 2009

[4] Charles E. Till, Yoon IL Chang, “Plentiful Energy,” CreateSpace, 2011

[5] Leonard J. Koch, “EBR-II,”

[6] Argonne National Laboratory, “EBR-II System Design Descriptions,” Volume II, Chapter 2, 1971

[7] T. Fei, A. Mohamed, T. K. Kim, “Neutronics Benchmark Specifications for EBR-II Shutdown Heat Removal Test SHRT-45-R,” Argonne National Laboratory, Revision 1, 2013

[8] Merriam-Webster, “Benchmark,” http://www.merriam-webster.com/dictionary/benchmark

[9] Chad L. Pope, Edward Lum, “Experimental Breeder Reactor II Benchmark Evaluation,”

[10] James J. Duderstadt, Louis J. Hamilton, “Nuclear Reactor Analysis,” John Wiley & Sons, 1976

[11] Chad L. Pope, “Spent Nuclear Fuel Assembly Inspection Using Neutron Computed Tomography,” Idaho State University, 2010

[12] Chad L. Pope, Michael J. Lineberry, “Comparison of Measured and Monte Carlo Results for Neutron Beam Transmission Through an Irradiated Nuclear Fuel Assembly,” Idaho National Laboratory, Idaho State University, 2012

[13] Michelbacher, J. A.; Baily, C. E.; Baird, D. K.; Henslee, S. P.; Knight, C. J.; Rosenberg, K. E. “Shutdown and Closure of the Experimental Breeder Reactor II,” Argonne National Laboratory, ASME, 2002

Appendix A

Table 7: Integrated Nuclide Sensitivity Coefficients (Extended)

Nuclide	Reaction	Sensitivity	Std. Dev.	% Std. Dev.
^{235}U	nubar	9.6081E-01	1.12E-04	0.01%
^{235}U	fission	5.2769E-01	4.91E-04	0.09%
^{235}U	total	4.5810E-01	1.07E-03	0.23%
^{235}U	n,gamma	-9.2460E-02	1.06E-04	0.11%
^{235}U	capture	-9.2460E-02	1.06E-04	0.11%
^{56}Fe	scatter	5.7375E-02	8.36E-04	1.46%
^{56}Fe	elastic	5.1578E-02	8.03E-04	1.56%
^{56}Fe	total	4.6199E-02	8.39E-04	1.82%
^{23}Na	scatter	3.8391E-02	9.63E-04	2.51%
^{23}Na	total	3.7402E-02	9.63E-04	2.57%
^{23}Na	elastic	3.4656E-02	9.31E-04	2.69%
^{238}U	nubar	3.4056E-02	8.68E-06	0.03%
^{238}U	capture	-2.8369E-02	2.98E-05	0.10%
^{238}U	n,gamma	-2.8369E-02	2.98E-05	0.10%
^{235}U	scatter	2.2863E-02	5.62E-04	2.46%
^{52}Cr	scatter	2.1694E-02	3.00E-04	1.38%
^{238}U	fission	2.0981E-02	2.85E-05	0.14%
^{52}Cr	elastic	2.0947E-02	2.96E-04	1.41%
^{52}Cr	total	1.9385E-02	3.00E-04	1.55%
^{238}U	scatter	1.6967E-02	3.93E-04	2.31%
^{58}Ni	scatter	1.2758E-02	1.75E-04	1.38%
^{235}U	n,n'	1.2678E-02	4.20E-04	3.31%
^{58}Ni	elastic	1.2505E-02	1.74E-04	1.40%
^{56}Fe	capture	-1.1176E-02	9.00E-06	0.08%
^{238}U	elastic	1.1140E-02	1.29E-04	1.16%
^{56}Fe	n,gamma	-1.0961E-02	8.94E-06	0.08%
^{238}U	total	9.5798E-03	4.23E-04	4.41%
^{235}U	elastic	9.1233E-03	1.85E-04	2.03%
^{58}Ni	total	7.2591E-03	1.77E-04	2.44%

Nuclide	Reaction	Sensitivity	Std. Dev.	% Std. Dev.
^{54}Fe	scatter	6.0541E-03	1.32E-04	2.17%
^{54}Fe	elastic	5.9065E-03	1.31E-04	2.22%
^{56}Fe	n,n'	5.7857E-03	1.63E-04	2.81%
^{58}Ni	capture	-5.4989E-03	4.06E-06	0.07%
^{238}U	n,n'	5.4065E-03	2.93E-04	5.41%
^{60}Ni	scatter	4.3477E-03	8.81E-05	2.03%
^{60}Ni	elastic	4.2158E-03	8.77E-05	2.08%
^{54}Fe	total	4.0680E-03	1.32E-04	3.25%
^{55}Mn	scatter	3.8472E-03	1.03E-04	2.69%
^{23}Na	n,n'	3.7352E-03	1.16E-04	3.09%
^{239}Pu	nubar	3.6454E-03	4.28E-07	0.01%
^{60}Ni	total	3.4038E-03	8.84E-05	2.60%
^{55}Mn	elastic	3.3916E-03	1.02E-04	3.00%
^{58}Ni	n,gamma	-3.1992E-03	2.00E-06	0.06%
^{53}Cr	scatter	2.9884E-03	9.09E-05	3.04%
^{53}Cr	elastic	2.7730E-03	9.05E-05	3.26%
^{28}Si	scatter	2.6522E-03	4.66E-05	1.76%
^{28}Si	elastic	2.6176E-03	4.65E-05	1.77%
^{28}Si	total	2.5507E-03	4.66E-05	1.83%
^{55}Mn	capture	-2.5240E-03	4.58E-06	0.18%
^{55}Mn	n,gamma	-2.5206E-03	4.58E-06	0.18%
^{52}Cr	capture	-2.3087E-03	3.39E-06	0.15%
^{239}Pu	fission	2.2998E-03	1.63E-06	0.07%
^{52}Cr	n,gamma	-2.2650E-03	3.38E-06	0.15%
^{239}Pu	total	2.1443E-03	2.81E-06	0.13%
^{58}Ni	n,p	-2.1278E-03	3.20E-06	0.15%
^{57}Fe	scatter	2.0093E-03	7.76E-05	3.86%
^{54}Fe	capture	-1.9860E-03	1.63E-06	0.08%
^{57}Fe	elastic	1.8246E-03	6.43E-05	3.53%
^{101}Ru	capture	-1.7955E-03	2.77E-06	0.15%
^{101}Ru	n,gamma	-1.7954E-03	2.77E-06	0.15%
^{53}Cr	total	1.7374E-03	9.15E-05	5.27%
^{95}Mo	capture	-1.5018E-03	2.36E-06	0.16%
^{95}Mo	n,gamma	-1.5010E-03	2.36E-06	0.16%
^{57}Fe	total	1.4826E-03	7.79E-05	5.26%

Nuclide	Reaction	Sensitivity	Std. Dev.	% Std. Dev.
^{236}U	nubar	1.4143E-03	2.84E-07	0.02%
^{101}Ru	total	-1.3426E-03	1.20E-05	0.90%
^{55}Mn	total	1.3232E-03	1.09E-04	8.22%
^{103}Rh	capture	-1.2881E-03	2.32E-06	0.18%
^{103}Rh	n,gamma	-1.2879E-03	2.32E-06	0.18%
^{50}Cr	scatter	1.2736E-03	4.40E-05	3.45%
^{53}Cr	capture	-1.2510E-03	1.06E-06	0.08%
^{53}Cr	n,gamma	-1.2456E-03	1.06E-06	0.09%
^{50}Cr	elastic	1.1738E-03	4.38E-05	3.73%
^{54}Fe	n,gamma	-1.1661E-03	9.09E-07	0.08%
^{99}Ru	capture	-1.0900E-03	2.02E-06	0.19%
^{99}Ru	n,gamma	-1.0886E-03	2.02E-06	0.19%
^{103}Rh	total	-1.0061E-03	8.36E-06	0.83%
^{23}Na	capture	-9.8945E-04	1.43E-06	0.14%
^{60}Ni	capture	-9.4389E-04	6.67E-07	0.07%
^{60}Ni	n,gamma	-9.1959E-04	6.62E-07	0.07%
^{98}Mo	scatter	8.6301E-04	1.68E-05	1.94%
^{236}U	fission	8.5930E-04	9.59E-07	0.11%
^{99}Ru	total	-8.4214E-04	7.55E-06	0.90%
^{97}Mo	capture	-8.4170E-04	7.17E-07	0.09%
^{97}Mo	n,gamma	-8.4158E-04	7.17E-07	0.09%
^{95}Mo	total	-8.3524E-04	1.36E-05	1.63%

Table 8: Mixture Sensitivity Coefficients (Complete List)

Mixture	Mixture Name	Sensitivity	Std. Dev.	% Std. Dev.
6	Fuel	4.6387E-01	1.15E-03	0.25%
5	SS 304	4.5698E-02	6.91E-04	1.51%
2	Sodium	2.4314E-02	8.69E-04	3.57%
9	Empty Fuel Rods	2.3490E-02	4.12E-04	1.75%
3	SS 316	1.9099E-02	4.87E-04	2.55%
10	Lower Driver Shield	1.1366E-02	3.95E-04	3.47%
12	Upper Driver Shield	1.7796E-03	6.21E-05	3.49%
4	Depleted Uranium	1.5004E-03	1.15E-04	7.67%
11	Lower Driver Adapter	1.2413E-03	6.91E-05	5.57%
16	Control Rod Poison	-8.1849E-04	3.31E-05	4.04%
7	SS Reflector	3.9195E-04	7.59E-05	19.37%
13	Upper Adapter	5.6026E-05	6.06E-06	10.82%
14	Empty Blanket Rods	7.3256E-06	2.98E-07	4.06%
15	Lower Blanket Adapter	5.2220E-06	4.43E-07	8.48%

Table 9: Uncertainty Information

Nuclide Reaction	Nuclide Reaction	Uncertainty Contribution
^{235}U n,gamma	^{235}U n,gamma	2.1777E+00 ± 1.3730E-03
^{235}U fission	^{235}U fission	2.1155E-01 ± 9.2017E-06
^{235}U elastic	^{235}U n,gamma	1.5587E-01 ± 1.0099E-04
^{235}U nubar	^{235}U nubar	1.4088E-01 ± 5.1463E-07
^{56}Fe elastic	^{56}Fe elastic	1.2223E-01 ± 4.4904E-05
^{235}U n,n'	^{235}U n,n'	1.2156E-01 ± 1.3147E-04
^{23}Na elastic	^{23}Na elastic	1.0730E-01 ± 8.8504E-05
^{52}Cr elastic	^{52}Cr elastic	8.5048E-02 ± 2.8297E-05
^{235}U elastic	^{235}U n,n'	-7.0090E-02 ± 2.1192E-05
^{56}Fe n,gamma	^{56}Fe n,gamma	6.7469E-02 ± 9.1286E-07
^{238}U n,n'	^{238}U n,n'	5.5689E-02 ± 6.0550E-05
^{235}U chi	^{235}U chi	5.2470E-02 ± 3.6921E-06
^{238}U elastic	^{238}U n,n'	-5.0369E-02 ± 1.7511E-05
^{238}U nubar	^{238}U nubar	4.0286E-02 ± 8.4555E-08
^{23}Na n,n'	^{23}Na n,n'	3.8488E-02 ± 1.2579E-05
^{23}Na elastic	^{23}Na n,n'	-3.7930E-02 ± 8.0968E-06
^{238}U n,gamma	^{238}U n,gamma	3.2808E-02 ± 3.0464E-07
^{238}U elastic	^{238}U elastic	2.8222E-02 ± 1.9693E-06
^{235}U elastic	^{235}U elastic	2.5963E-02 ± 3.0090E-06
^{236}U fission	^{236}U fission	2.5047E-02 ± 1.2702E-07
^{54}Fe elastic	^{54}Fe elastic	2.4942E-02 ± 2.9997E-06
^{95}Mo n,gamma	^{95}Mo n,gamma	2.1142E-02 ± 8.1725E-08
^{56}Fe elastic	^{56}Fe n,n'	-1.9567E-02 ± 1.4752E-06
^{58}Ni elastic	^{58}Ni elastic	1.9133E-02 ± 9.3405E-07
^{235}U elastic	^{235}U fission	-1.9044E-02 ± 6.7817E-07
^{55}Mn elastic	^{55}Mn elastic	1.8696E-02 ± 1.7591E-06
^{57}Fe elastic	^{57}Fe elastic	1.8614E-02 ± 2.4027E-06
^{52}Cr n,gamma	^{52}Cr n,gamma	1.7971E-02 ± 9.2414E-08
^{58}Ni n,gamma	^{58}Ni n,gamma	1.7875E-02 ± 6.0897E-08
^{235}U fission	^{235}U n,gamma	1.6715E-02 ± 3.4444E-07
^{56}Fe n,n'	^{56}Fe n,n'	1.5914E-02 ± 2.2140E-06
^{54}Fe n,gamma	^{54}Fe n,gamma	1.4137E-02 ± 5.4835E-08
^{101}Ru n,gamma	^{101}Ru n,gamma	1.2479E-02 ± 4.6964E-08
^{238}U fission	^{238}U fission	1.0964E-02 ± 3.1550E-08

Nuclide Reaction	Nuclide Reaction	Uncertainty Contribution
^{102}Ru n,gamma	^{102}Ru n,gamma	1.0430E-02 ± 2.4900E-08
^{53}Cr elastic	^{53}Cr elastic	9.9930E-03 ± 6.6967E-07
^{97}Mo n,gamma	^{97}Mo n,gamma	9.8642E-03 ± 1.7646E-08
^{56}Fe elastic	^{56}Fe n,gamma	9.4851E-03 ± 3.0730E-07
^{99}Ru n,gamma	^{99}Ru n,gamma	9.3255E-03 ± 2.5913E-08
^{55}Mn n,gamma	^{55}Mn n,gamma	9.1162E-03 ± 4.6617E-08
^{23}Na n,gamma	^{23}Na n,gamma	8.8720E-03 ± 3.5519E-08
^{60}Ni elastic	^{60}Ni elastic	8.7272E-03 ± 2.2725E-07
^{53}Cr n,gamma	^{53}Cr n,gamma	7.7313E-03 ± 1.8275E-08
^{62}Ni elastic	^{62}Ni elastic	7.6335E-03 ± 3.6971E-07
^{103}Rh n,gamma	^{103}Rh n,gamma	7.3632E-03 ± 2.2189E-08
^{57}Fe n,gamma	^{57}Fe n,gamma	7.3305E-03 ± 2.4553E-08
^{100}Ru n,gamma	^{100}Ru n,gamma	6.9701E-03 ± 1.0045E-08
^{96}Mo n,gamma	^{96}Mo n,gamma	6.9351E-03 ± 9.3193E-09
^{238}U n,2n	^{238}U n,2n	6.3219E-03 ± 2.0359E-07
^{98}Mo n,gamma	^{98}Mo n,gamma	6.2446E-03 ± 6.4435E-09

Appendix B

06/22/2015 email from author to Oak Ridge National Laboratory (ORNL):

Hello,

I performed a sensitivity analysis using Tsunami-3D for my thesis, and would like to provide a brief explanation about how KENO-VI performs the adjoint flux calculation. Unfortunately, I have no idea how it does this. For the forward flux calculation I understand that neutrons are tracked through the system, from birth until leakage or absorption. How does it work for the adjoint flux? If you could describe it to me, or point me to a specific section in the scale manual where this is adequately described, it would be greatly appreciated.

Thank you,

Shawn Seegmiller
Idaho State University
Nuclear Engineering

06/30/2015 response from ORNL to author:

Hello,

*The SCALE manual doesn't describe solving the adjoint eigenvalue in any detail. The equation is the same form as the forward equation, and, for a multigroup implementation, can be solved using the same procedures. For a heuristic view, think of a fission event as a source (the event, not the neutrons produced). For the adjoint flux, a particle is born at the event and followed back until it reaches the point at which the neutron producing the event was born. This adjoint particle then undergoes something like an adjoint fission(the neutron born there was produced by a previous generation fission event). To simulate this in multigroup, it is only necessary to invert the group structure and the scattering matrix, and to interchange nu*sigma fission and chi, normalizing nu*sigma fission to 1.0, and multiplying chi by the normalization factor. Unfortunately, interchanging the scattering matrix leads to the cross sections not being in balance, which leads to large variances in the Monte Carlo calculation. This is why the adjoint calculation runs many more histories, and usually takes most of the time in the tsunami calculations. The basic adjoint equation should be derived in any good neutronics text book. I hope this helps you.*

SCALE Help

Appendix C

TSUNAMI Input File

```
'Input generated by GeeWiz SCALE 6.1 Compiled on Mon Jun  6 11:04:33 2011
=tsunami-3d-k6
ebr-ii
v7-238
read composition
 u         1 1 616
                      92235 67
                      92238 33   end
 sodium     2 den=0.87 1 616   end
 ss316      3 1 616   end
 uranium    4 1 616
                      92235 0.2
                      92238 99.8   end
 ss304      5 1 616   end
 wtptu-5s       6  12.43  17
                      92235 60.71717
                      92238 31.97175
                      40000 0.127443
                      42000 3.135096
                      44000 2.497881
                      45000 0.35684
                      46000 0.242142
                      41000 0.012744
                      57139 0.119157
                      93237 0.006233
                      60148 0.033493
                      94238 6.9e-05
                      94239 0.164535
                      94240 0.000645
                      94241 2e-06
                      92234 0.00233
```

```
                92236 0.612469
            1 616   end
wtptssreflkt    7  6.929  8
                6000 0.079
                14000 0.982
                15000 0.044
                24000 18.659
                25055 1.964
                26000 67.147
                28000 9.329
                11000 1.796
            1 616
                15031 100   end
wtptdublkt     8  13.232  10
                6000 0.008
                14000 0.105
                15031 0.005
                24000 2.01
                25055 0.212
                26000 7.234
                28000 1.005
                92235 0.176
                92238 87.849
                11000 1.396
            1 616   end
wtptemtydrivrrds 9  2.233  9
                6000 0.064
                14000 0.802
                15031 0.036
                25055 1.604
                26000 52.434
                28000 9.625
                42000 2.005
                11000 19.795
                24000 13.635
```

1 616 end

wtptlowdrvrshld 10 4.992 8

6000 0.074

14000 0.927

15031 0.042

24000 17.619

25055 1.855

26000 63.405

28000 8.81

11000 7.268

1 616 end

wtptlowdrvradtr 11 2.341 8

6000 0.056

14000 0.706

15031 0.032

24000 13.407

25055 1.411

26000 48.246

28000 6.703

11000 29.439

1 616 end

wtptupdrvrshld 12 4.405 8

6000 0.072

14000 0.901

15031 0.041

24000 17.124

25055 1.802

26000 61.623

28000 8.562

11000 9.875

1 616 end

wtptupadptr 13 1.344 8

6000 0.032

14000 0.396

15031 0.018

```
                    24000 7.522
                    25055 0.792
                    26000 27.07
                    28000 3.761
                    11000 60.409
                1 616   end
wtptemtyblktrds 14  1.582  8
                    6000 0.071
                    14000 0.883
                    15031 0.04
                    24000 16.785
                    25055 1.767
                    26000 60.402
                    28000 8.392
                    11000 11.66
                1 616   end
wtptlowblktadptr 15  2.821  8
                    6000 0.062
                    14000 0.777
                    15031 0.035
                    24000 14.758
                    25055 1.553
                    26000 53.11
                    28000 7.379
                    11000 22.326
                1 616   end
wtptpoison      16  2.726  9
                    6000 6.975
                    14000 0.53
                    15031 0.024
                    24000 10.072
                    25055 1.06
                    26000 36.247
                    28000 5.036
                    11000 15.096
```

```
                    5000 24.96
                1 616   end
end composition
read celldata
 latticecell triangpitch fuelr=0.196221 6 cladr=0.22098 3 hpitch=0.28298 2 end
end celldata
read parameter
 gen=250
 npg=10000
 htm=yes
 ask=200
 apg=1000000
 abk=80000
 agn=1000
end parameter
read geometry
unit 1
com="driver fuel rod"
 cylinder 1  0.196221  118.9805  -114.2995   origin  x=-0.06 y=0 z=0
 cylinder 3  0.22098  118.9805  -114.2995   origin  x=-0.06 y=0 z=0
 rhexprism 5  0.28298  118.9805  -114.2995
 cylinder 6  0.06223  118.9805  -114.2995   origin  x=0.22321 y=0 z=0
 media 6 1 1
 media 3 1 -1 3
 media 3 1 6
 media 2 1 5 -6 -3
 boundary 5
unit 50
com="global unit 2 references array 1 - driver subassembly"
 hexprism 3   2.8067    36.65       0
 array 1 3  place 7 7 1 0.06 0 0
 hexprism 4   2.9083    36.65       0
 hexprism 5  2.94645    36.65       0
 hexprism 6  2.94645   61.727    36.65
 hexprism 7  2.94645  104.733   61.727
```

```
 hexprism 8  2.94645  118.9805  104.733
 hexprism 9  2.94645        0  -62.387
 hexprism 10  2.94645  -62.387  -114.2995
 hexprism 11  2.94645  118.9805  -114.2995
 media 3 1 -3 4
 media 2 1 -4 5
 media 9 1 6
 media 12 1 7
 media 13 1 8
 media 10 1 9
 media 11 1 10
 boundary 11
unit 2
com="sodium void - driver subassembly"
 rhexprism 1  0.28298  118.9805  -114.2995
 media 2 1 1
 boundary 1
unit 3
com="blanket rod"
 cylinder 1  0.55499  118.9805  -114.2995
 cylinder 2  0.58041  118.9805  -114.2995
 cylinder 3  0.62611  118.9805  -114.2995
 rhexprism 4   0.6275  118.9805  -114.2995
 media 4 1 1
 media 2 1 -1 2
 media 5 1 -2 3
 media 2 1 -3 4
 boundary 4
unit 60
com="blanket subassembly"
 hexprism 3   2.8067  83.79998  -55.90002
 hexprism 4   2.9083  83.79998  -55.90002
 array 2 3  place 4 4 1 0 0 0
 hexprism 5  2.94645  83.79998  -55.90002
 hexprism 6  2.94645  -55.90002  -114.2995
```

```
 hexprism 7  2.94645  98.62798  83.79998
 hexprism 8  2.94645  118.9805  98.62798
 hexprism 9  2.94645  118.9805  -114.2995
 media 5 1 -3 4
 media 2 1 -4 5
 media 15 1 6
 media 14 1 7
 media 13 1 8
 boundary 9
unit 4
com="sodium void - blanket subassembly"
 rhexprism 1   0.6275  118.9805  -114.2995
 media 2 1 1
 boundary 1
unit 70
com="high worth control rod subassembly"
 hexprism 6     2.32    36.65       0
 hexprism 7     2.42    36.65       0
 hexprism 8   2.8067    36.65       0
 hexprism 9   2.9083    36.65       0
 array 3 6  place 6 6 1 0 0 0
 hexprism 10  2.94645    36.65       0
 hexprism 11  2.94645       0  -71.983
 hexprism 12  2.94645    53.47    36.65
 hexprism 13  2.94645  118.9805    53.47
 hexprism 15  2.94645  118.9805  -114.2995
 hexprism 16  2.94645  -71.983  -114.2995
 media 5 1 -6 7
 media 3 1 -8 9
 media 2 1 -7 8
 media 2 1 -9 10
 media 11 1 11
 media 9 1 12
 media 16 1 13
 media 2 1 16
```

```
 boundary 15
unit 80
com="half worth driver subassembly"
 hexprism 3   2.8067    36.65       0
 array 4 3  place 7 7 1 0.06 0 0
 hexprism 4   2.9083    36.65       0
 hexprism 5  2.94645    36.65       0
 hexprism 6  2.94645  -62.387  -114.2995
 hexprism 7  2.94645       0  -62.387
 hexprism 8  2.94645   61.727    36.65
 hexprism 9  2.94645  104.733   61.727
 hexprism 10  2.94645  118.9805  104.733
 hexprism 11  2.94645  118.9805  -114.2995
 media 3 1 -3 4
 media 2 1 -4 5
 media 11 1 6
 media 10 1 7
 media 9 1 8
 media 12 1 9
 media 13 1 10
 boundary 11
unit 5
com="stainless stee 316 dummy rod"
 cylinder 3  0.22098  118.9805  -114.2995   origin  x=-0.06 y=0 z=0
 rhexprism 5  0.28298  118.9805  -114.2995
 cylinder 6  0.06223  118.9805  -114.2995   origin  x=0.22321 y=0 z=0
 media 3 1 3
 media 3 1 6
 media 2 1 5 -6 -3
 boundary 5
unit 200
com="core"
 cylinder 1      15    34.29       0
 array 5 1  place 4 4 1 0 0 0
 boundary 1
```

```
unit 150
com="sodium void - outside of core"
 hexprism 1  2.94645  118.9805  -114.2995
 media 2 1 1
 boundary 1
unit 90
com="ss reflector subassembly"
 hexprism 1  2.61874  98.3805  -57.6295
 hexprism 2   2.8067  98.3805  -57.6295
 hexprism 3   2.9083  98.3805  -57.6295
 hexprism 4  2.94645  98.3805  -57.6295
 hexprism 5  2.94645  -57.6295  -114.2995
 hexprism 6  2.94645  118.9805  98.3805
 hexprism 7  2.94645  118.9805  -114.2995
 media 5 1 1
 media 2 1 -1 2
 media 5 1 -2 3
 media 2 1 -3 4
 media 15 1 5
 media 13 1 6
 boundary 7
unit 6
com="dummy ss rod"
 cylinder 1  0.641985  118.9805  -114.2995
 rhexprism 4  0.935567  118.9805  -114.2995
 media 5 1 1
 media 2 1 -1 4
 boundary 4
unit 100
com="ss dummy subassembly"
 hexprism 3   2.8067  98.0615  -53.8305
 hexprism 4   2.9083  98.0615  -53.8305
 array 6 3  place 3 3 1 0 0 0
 hexprism 5  2.94645  98.0615  -53.8305
 hexprism 6  2.94645  -53.8305  -114.2995
```

```
 hexprism 7  2.94645  118.9805  98.0615
 hexprism 8  2.94645  118.9805  -114.2995
 media 5 1 -3 4
 media 2 1 -4 5
 media 11 1 6
 media 13 1 7
 boundary 8
unit 7
com="ss dummy rod sodium void"
 rhexprism 4  0.935567  118.9805  -114.2995
 media 2 1 4
 boundary 4
unit 110
com="xx09 subassembly"
 hexprism 6     2.32  38.7505   2.1005
 hexprism 7     2.42  38.7505   2.1005
 hexprism 8   2.8067  38.7505   2.1005
 hexprism 9   2.9083  38.7505   2.1005
 array 7 6  place 6 6 1 0 0 0
 hexprism 10  2.94645  38.7505   2.1005
 hexprism 11  2.94645   2.1005  -114.2995
 hexprism 12  2.94645  63.3005  38.7505
 hexprism 13  2.94645  118.9805  63.3005
 hexprism 14  2.94645  118.9805  -114.2995
 media 5 1 -6 7
 media 5 1 -8 9
 media 2 1 -7 8
 media 2 1 -9 10
 media 11 1 11
 media 9 1 12
 media 13 1 13
 boundary 14
unit 120
com="xx10 subassembly"
 hexprism 6     2.32  63.3005   2.1005
```

```
 hexprism 7     2.42  63.3005   2.1005
 hexprism 8   2.8067  63.3005   2.1005
 hexprism 9   2.9083  63.3005   2.1005
 array 8 6  place 4 4 1 0 0 0
 hexprism 10  2.94645  63.3005   2.1005
 hexprism 11  2.94645   2.1005  -114.2995
 hexprism 12  2.94645  118.9805  63.3005
 hexprism 13  2.94645  118.9805  -114.2995
 media 5 1 -6 7
 media 5 1 -8 9
 media 2 1 -7 8
 media 2 1 -9 10
 media 11 1 11
 media 13 1 12
 boundary 13
unit 8
com="xx10 rods"
 cylinder 1   0.4405  118.9805  -114.2995
 cylinder 2    0.062  118.9805  -114.2995   origin  x=0.5025 y=0 z=0
 rhexprism 3   0.5025  118.9805  -114.2995
 media 3 1 1
 media 3 1 2
 media 2 1 -1 -2 3
 boundary 3
unit 9
com="sodium void - xx10"
 rhexprism 3   0.5025  118.9805  -114.2995
 media 2 1 3
 boundary 3
unit 130
com="xy-16 subassembly"
 hexprism 6     2.32    34.29       0
 hexprism 7     2.42    34.29       0
 hexprism 8   2.8067    34.29       0
 hexprism 9   2.9083    34.29       0
```

```
 array 9 6  place 6 6 1 0.06 0 0
 hexprism 10  2.94645    34.29       0
 hexprism 11  2.94645  -62.387  -114.2995
 hexprism 12  2.94645       0  -62.387
 hexprism 13  2.94645   61.727    34.29
 hexprism 14  2.94645  104.733   61.727
 hexprism 15  2.94645  118.9805  104.733
 hexprism 16  2.94645  118.9805  -114.2995
 media 5 1 -6 7
 media 5 1 -8 9
 media 2 1 -7 8
 media 2 1 -9 10
 media 11 1 11
 media 10 1 12
 media 9 1 13
 media 12 1 14
 media 13 1 15
 boundary 16
unit 10
com="ss 304 dummy rod"
 cylinder 3  0.22098  118.9805  -114.2995   origin  x=-0.06 y=0 z=0
 rhexprism 5  0.28298  118.9805  -114.2995
 cylinder 6  0.06223  118.9805  -114.2995   origin  x=0.22321 y=0 z=0
 media 5 1 3
 media 3 1 6
 media 2 1 5 -6 -3
 boundary 5
unit 160
com="homogeneous reflector blanket subassembly"
 hexprism 1  2.94645  98.3805  -57.6295
 hexprism 2  2.94645  -57.6295  -114.2995
 hexprism 3  2.94645  118.9805  98.3805
 hexprism 4  2.94645  118.9805  -114.2995
 media 7 1 1
 media 15 1 2
```

```
 media 13 1 3
 boundary 4
unit 210
com="better core"
 rhexprism 1  34.0227  118.9805  -114.2995
 rhexprism 2  51.03401  108.3905  -47.6195
 cylinder 4  81.6545  83.79998  -55.90002
 array 10 1  place 8 8 1 0 0 0
 rhexprism 5  51.03401  -47.6195  -114.2995
 rhexprism 6  51.03401  118.9805  108.3905
 cylinder 7  81.6545  -55.90002  -114.2995
 cylinder 8  81.6545  98.62798  83.79998
 cylinder 9  81.6545  118.9805  98.62798
 cylinder 10  81.6545  118.9805  -114.2995
 rhexprism 11  51.03401  118.9805  -114.2995
 media 7 1 -1 2
 media 15 1 -1 5
 media 13 1 -1 6
 media 8 1 -11 4
 media 15 1 -11 7
 media 14 1 -11 8
 media 13 1 -11 9
 boundary 10
unit 75
com="safety rod subassembly"
 hexprism 6     2.32    36.65       0
 hexprism 7     2.42    36.65       0
 hexprism 8   2.8067    36.65       0
 hexprism 9   2.9083    36.65       0
 array 3 6  place 6 6 1 0 0 0
 hexprism 10  2.94645    36.65       0
 hexprism 11  2.94645    -38.1    -97.6
 hexprism 12  2.94645       0    -38.1
 hexprism 13  2.94645   61.715    36.65
 hexprism 14  2.94645   92.215   61.715
```

hexprism 15 2.94645 118.9805   92.215

hexprism 16 2.94645 118.9805 -114.2995

hexprism 17 2.94645   -97.6 -114.2995

media 5 1 -6 7

media 3 1 -8 9

media 2 1 -7 8

media 2 1 -9 10

media 11 1 11

media 7 1 12

media 9 1 13

media 7 1 14

media 13 1 15

media 2 1 17

boundary 16

unit 72

com="poison hwcr subassembly"

hexprism 6   2.32   -46.25   -82.9

hexprism 7   2.42   -46.25   -82.9

hexprism 8   2.8067   -46.25   -82.9

hexprism 9   2.9083   -46.25   -82.9

array 3 6 place 6 6 1 0 0 0

hexprism 10 2.94645   -46.25   -82.9

hexprism 11 2.94645   -82.9 -114.2995

hexprism 12 2.94645   -29.43   -46.25

hexprism 13 2.94645   63.72   -29.43

hexprism 15 2.94645 118.9805 -114.2995

hexprism 16 2.94645   82.66   63.72

hexprism 17 2.94645 118.9805   82.66

media 5 1 -6 7

media 3 1 -8 9

media 2 1 -7 8

media 2 1 -9 10

media 11 1 11

media 9 1 12

media 16 1 13

```
 media 13 1 16
 media 2 1 17
 boundary 15
unit 73
com="lowered hwcr subassembly"
 hexprism 6     2.32       0   -36.65
 hexprism 7     2.42       0   -36.65
 hexprism 8   2.8067       0   -36.65
 hexprism 9   2.9083       0   -36.65
 array 3 6  place 6 6 1 0 0 0
 hexprism 10  2.94645       0   -36.65
 hexprism 11  2.94645   -36.65  -108.633
 hexprism 12  2.94645    16.82       0
 hexprism 13  2.94645   109.97    16.82
 hexprism 15  2.94645  118.9805  -114.2995
 hexprism 16  2.94645  -108.633  -114.2995
 hexprism 17  2.94645  118.9805   109.97
 media 5 1 -6 7
 media 3 1 -8 9
 media 2 1 -7 8
 media 2 1 -9 10
 media 11 1 11
 media 9 1 12
 media 16 1 13
 media 2 1 16
 media 13 1 17
 boundary 15
unit 74
com="partially lowered hwcr subassembly"
 hexprism 6     2.32   7.6454  -29.0046
 hexprism 7     2.42   7.6454  -29.0046
 hexprism 8   2.8067   7.6454  -29.0046
 hexprism 9   2.9083   7.6454  -29.0046
 array 3 6  place 6 6 1 0 0 0
 hexprism 10  2.94645   7.6454  -29.0046
```

```
 hexprism 11  2.94645  -29.0046  -100.9876
 hexprism 12  2.94645  24.4654   7.6454
 hexprism 13  2.94645  118.9805  24.4654
 hexprism 15  2.94645  118.9805  -114.2995
 hexprism 16  2.94645  -100.9876  -114.2995
 media 5 1 -6 7
 media 3 1 -8 9
 media 2 1 -7 8
 media 2 1 -9 10
 media 11 1 11
 media 9 1 12
 media 16 1 13
 media 2 1 16
 boundary 15
unit 76
com="lowered safety rod subassembly"
 hexprism 6     2.32       0   -36.65
 hexprism 7     2.42       0   -36.65
 hexprism 8   2.8067       0   -36.65
 hexprism 9   2.9083       0   -36.65
 array 3 6  place 6 6 1 0 0 0
 hexprism 10  2.94645       0   -36.65
 hexprism 11  2.94645   -74.75  -114.2995
 hexprism 12  2.94645   -36.65   -74.75
 hexprism 13  2.94645   25.065       0
 hexprism 14  2.94645   55.565   25.065
 hexprism 15  2.94645  118.9805   55.565
 hexprism 16  2.94645  118.9805  -114.2995
 media 5 1 -6 7
 media 3 1 -8 9
 media 2 1 -7 8
 media 2 1 -9 10
 media 11 1 11
 media 7 1 12
 media 9 1 13
```

```
 media 7 1 14
 media 13 1 15
 boundary 16
global unit 211
com="non homogeneous core"
 cylinder 10  81.6545  118.9805  -114.2995
 array 12 10  place 16 17 1 0 0 0
 boundary 10
end geometry
read array
ara=1 nux=13 nuy=13 nuz=1 typ=rhexagonal
 com='driver assembly'
 fill
   1   1   1   1   1   2   2   2   1   1   1   1   1
   1   1   1   2   2   1   1   1   2   2   1   1   1
   1   2   2   1   1   1   1   1   1   1   2   2   1
   2   1   1   1   1   1   1   1   1   1   1   1   2
   2   1   1   1   1   1   1   1   1   1   1   1   2
   2   1   1   1   1   1   1   1   1   1   1   1   2
   2   1   1   1   1   1   1   1   1   1   1   1   2
   2   1   1   1   1   1   1   1   1   1   1   1   2
   2   1   1   1   1   1   1   1   1   1   1   1   2
   2   2   1   1   1   1   1   1   1   1   1   2   2
   1   1   2   2   1   1   1   1   1   2   2   1   1
   1   1   1   1   2   2   1   2   2   1   1   1   1
   1   1   1   1   1   1   2   1   1   1   1   1   1  end fill
ara=2 nux=7 nuy=7 nuz=1 typ=rhexagonal
 com='du blanket assembly'
 fill
   4   4   4   4   4   4   4
   4   4   4   3   4   4   4
   4   3   3   3   3   3   4
   4   3   3   3   3   3   4
   4   3   3   3   3   3   4
   4   4   3   3   3   4   4
```

```
   4   4   4   4   4   4   4  end fill
ara=3 nux=11 nuy=11 nuz=1 typ=rhexagonal
 com='hwcr/safety rod assembly'
 fill
   1   1   1   1   1   2   1   1   1   1   1
   1   1   1   2   2   1   2   2   1   1   1
   1   2   2   1   1   1   1   1   2   2   1
   2   1   1   1   1   1   1   1   1   1   2
   2   1   1   1   1   1   1   1   1   1   2
   2   1   1   1   1   1   1   1   1   1   2
   2   1   1   1   1   1   1   1   1   1   2
   2   1   1   1   1   1   1   1   1   1   2
   2   2   1   1   1   1   1   1   1   2   2
   1   1   2   2   1   1   1   2   2   1   1
   1   1   1   1   2   2   2   1   1   1   1  end fill
ara=4 nux=13 nuy=13 nuz=1 typ=rhexagonal
 com=''
 fill
   1   1   1   1   1   2   2   2   1   1   1   1   1
   1   1   1   2   2   5   1   1   2   2   1   1   1
   1   2   2   5   1   1   5   1   5   5   2   2   1
   2   5   1   1   5   1   5   5   1   5   1   1   2
   2   1   5   1   5   5   1   5   1   1   5   5   2
   2   1   5   5   1   5   1   1   5   5   1   5   2
   2   5   1   5   1   1   5   5   1   5   1   1   2
   2   5   1   1   5   5   1   5   1   1   5   1   2
   2   1   5   5   1   5   1   1   5   1   5   5   2
   2   2   1   5   1   1   5   1   5   5   1   2   2
   1   1   2   2   5   1   5   5   1   2   2   1   1
   1   1   1   1   2   2   1   2   2   1   1   1   1
   1   1   1   1   1   1   2   1   1   1   1   1   1  end fill
ara=5 nux=7 nuy=7 nuz=1 typ=shexagonal
 com=''
 fill
 150  150  150  150  150  150  150
```

150 150 90 100 120 150 150

150 150 110 50 50 80 150

150 100 50 50 50 80 150

150 150 60 50 50 130 150

150 150 120 60 70 150 150

150 150 150 150 150 150 150 end fill

ara=6 nux=5 nuy=5 nuz=1 typ=rhexagonal

com=''

fill

6 7 7 7 6

7 6 6 6 7

7 6 6 6 7

7 7 6 7 7

6 6 7 6 6 end fill

ara=7 nux=11 nuy=11 nuz=1 typ=rhexagonal

com=''

fill

1 1 1 1 1 2 1 1 1 1 1

1 1 1 2 2 1 2 2 1 1 1

1 2 2 1 1 1 1 1 2 2 1

2 1 1 1 1 1 1 1 1 1 2

2 1 1 5 1 1 1 1 1 1 2

2 1 1 1 1 1 1 1 1 1 2

2 1 1 1 1 1 1 1 1 1 2

2 1 1 1 1 1 5 1 1 1 2

2 2 1 1 1 1 1 1 1 2 2

1 1 2 2 1 1 1 2 2 1 1

1 1 1 1 2 2 2 1 1 1 1 end fill

ara=8 nux=7 nuy=7 nuz=1 typ=rhexagonal

com=''

fill

9 9 9 9 9 9 9

9 9 9 8 9 9 9

9 8 8 8 8 8 9

9 8 8 8 8 8 9

```
  9   8   8   8   8   8   9
  9   9   8   8   8   9   9
  9   9   9   9   9   9   9  end fill
ara=9 nux=11 nuy=11 nuz=1 typ=rhexagonal
 com=''
 fill
  2   2   2   2   2   2   2   2   2   2   2
  2   2   2   2   2  10   2   2   2   2   2
  2   2   2  10  10  10  10  10   2   2   2
  2  10  10  10  10  10  10  10  10  10   2
  2  10  10  10  10  10  10  10  10  10   2
  2  10  10  10  10  10  10  10  10  10   2
  2  10  10  10  10  10  10  10  10  10   2
  2  10  10  10  10  10  10  10  10  10   2
  2   2  10  10  10  10  10  10  10   2   2
  2   2   2   2  10  10  10   2   2   2   2
  2   2   2   2   2   2   2   2   2   2   2  end fill
ara=10 nux=15 nuy=15 nuz=1 typ=shexagonal
 com='overall core model'
 fill
 160 160 160 160 160 160 160 160 160 160 160 160 160 160 160
 160 160 160 160  90  90  50  50  90  90  50 160 160 160 160
 160 160 160 160  90  50  50  80  50  50  50  90 160 160 160
 160 160 160  90  50  70  50  70  50  70  50  90 160 160 160
 160 160 160  50  80  50  50  50  50  50  50  50  50 160 160
 160 160  50  50 130  50  50  80  50  50 110  50  50 160 160
 160 160  90  50  50  50 100 100  80  80 130  50  50  90 160
 160  90  50  70  50  75  80  80 100  75  50  70  50  90 160
 160 160  90  50  50  50  80 100  80  80  50  50  80  90 160
 160 160  90  50 100  50  50 100  50  50  70  50  90 160 160
 160 160 160  90  50  50  50  50  50  50  50  50  50 160 160
 160 160 160  80  50  70  50  70  50 120  50  50 160 160 160
 160 160 160 160  50  50  50  50  80  50  50  90 160 160 160
 160 160 160 160  50  90  50  90  50  90  50 160 160 160 160
 160 160 160 160 160 160 160 160 160 160 160 160 160 160 160  end fill
```

ara=12 nux=31 nuy=33 nuz=1 typ=shexagonal gbl=12

com=''

fill

150 150 150 150 150 150 150 150 150 150 150 150 150 150 150 150 150 150 150 150 150 150 150 150 150 150 150 150 150 150 150 150 150

150 150 150 150 150 150 150 150 150 150 150 150 150 90 60 60 90 150 150 150 150 150 150 150 150 150 150 150 150 150 150 150 150

150 150 150 150 150 150 150 150 150 150 150 60 60 60 90 60 60 60 60 60 60 60 150 150 150 150 150 150 150 150 150 150 150

150 150 150 150 150 150 150 150 150 60 60 90 60 90 60 60 60 60 90 60 60 60 60 150 150 150 150 150 150 150 150 150 150

150 150 150 150 150 150 150 60 60 60 60 90 60 60 60 60 60 60 60 60 90 60 60 60 150 150 150 150 150 150 150 150 150

150 150 150 150 150 150 60 90 60 60 60 60 60 60 60 60 60 60 60 60 60 60 60 90 60 150 150 150 150 150 150 150 150

150 150 150 150 150 150 60 60 90 60 60 60 60 60 60 60 60 60 60 60 60 60 60 60 60 60 60 150 150 150 150 150 150

150 150 150 150 90 60 60 60 60 60 90 90 90 90 90 90 90 90 90 90 60 60 60 60 90 90 150 150 150 150 150

150 150 150 150 60 60 60 60 60 60 90 90 90 90 90 90 90 90 90 90 90 60 60 60 60 60 60 150 150 150 150

150 150 150 90 60 60 60 60 60 90 90 90 90 90 90 90 90 90 90 90 90 90 60 60 60 60 60 60 150 150 150 150

150 150 150 90 60 60 60 60 60 90 90 90 90 90 50 50 90 90 50 90 90 90 60 60 60 60 60 90 150 150 150

150 150 150 90 60 60 60 60 90 90 90 90 50 50 80 50 50 50 90 90 90 90 60 60 90 60 60 150 150 150 150

150 150 150 60 60 60 60 60 90 90 90 90 50 70 50 70 50 70 50 90 90 90 90 60 60 60 60 60 150 150 150

150 150 60 60 60 60 60 90 90 90 50 80 50 50 50 50 50 50 50 90 90 90 60 60 60 60 60 150 150 150

150 150 60 90 90 60 60 90 90 90 50 50 130 50 50 80 50 50 110 50 50 90 90 90 60 60 60 60 60 150 150

150 150 60 60 60 60 90 90 90 90 50 50 50 100 100 80 80 130 50 50 90 90 90 90 60 60 60 60 150 150 150

150 150 60 90 60 60 90 90 90 90 50 70 50 75 80 80 100 75 50 70 50 90 90 90 90 60 60 60 90 150 150

150 150 60 60 60 60 90 90 90 90 50 50 50 80 100 80 80 50 50 80 90 90 90 90 60 60 60 60 150 150 150

150 150 60 90 60 60 60 90 90 90 90 50 100 50 50 100 50 50 70 50 90 90 90 90 60 60 90 60 60 150 150

150 150 60 60 60 60 60 90 90 90 90 50 50 50 50 50 50 50 50 50 90 90 90 60 60 60 60 60 150 150 150

150 150 150 60 60 60 60 60 90 90 90 80 50 70 50 70 50 120 50 50 90 90 90 60 60 60 60 150 150 150 150

150 150 150 60 60 60 60 60 90 90 90 50 50 50 50 80 50 50 90 90 90 90 60 60 60 60 60 150 150 150 150

150 150 150 90 60 60 60 60 60 90 90 90 50 90 50 90 50 90 50 90 90 90 60 60 90 60 60 60 150 150 150

150 150 150 60 60 60 60 60 60 90 90 90 90 90 90 90 90 90 90 90 90 90 90 60 60 60 60 60 60 150 150 150 150

150 150 150 150 60 60 60 60 60 60 90 90 90 90 90 90 90 90 90 90 90 90 90 60 60 60 60 60 90 150 150 150 150

150 150 150 150 60 60 60 60 60 60 90 90 90 90 90 90 90 90 90 90 90 90 90 60 60 60 60 60 60 150 150 150 150 150

150 150 150 150 150 150 60 60 90 60 60 60 60 60 60 60 60 60 60 60 60 60 60 60 60 60 150 150 150 150 150 150

150 150 150 150 150 150 60 60 60 60 60 60 60 60 60 60 60 60 60 60 60 60 60 60 60 60 60 150 150 150 150 150 150

150 150 150 150 150 150 150 60 60 60 60 60 60 60 60 60 60 60 60 60 60 60 60 60 60 60 60 150 150 150 150 150 150

150 150 150 150 150 150 150 150 60 90 90 60 60 60 60 60 60 60 60 60 90 60 150 150 150 150 150 150 150 150 150

150 150 150 150 150 150 150 150 150 150 60 60 60 60 60 60 60 60 60 60 60 150 150 150 150 150 150 150 150 150 150

```
 150 150 150 150 150 150 150 150 150 150 150 150 150  90  60  90  90 150 150 150 150 150 150 150 150 150 150 150 150 150

 150 150 150 150 150 150 150 150 150 150 150 150 150 150 150 150 150 150 150 150 150 150 150 150 150 150 150 150 150 150
150  end fill

end array

read plot

 scr=yes

 ttl='ebr ii blah'

 pic=mixtures

 xul=-81.6545

 yul=81.6545

 zul=5

 xlr=81.6545

 ylr=-81.6545

 zlr=5

 nax=5000

 clr=1 255 0 0

    2 0 0 205

    3 0 229 238

    4 0 238 0

    5 205 205 0

    6 238 0 0

    7 145 44 238

    8 150 150 150

    9 240 200 220

    10 0 191 255

    11 224 255 255

    12 0 255 127

    13 255 255 224

    14 255 0 0

    15 255 0 255

    16 67 110 238

 end color

 uax=1 vdn=-1

  end

end plot
```

```
read start
 nst=0
 xsm=-10
 xsp=10
 ysm=-10
 ysp=10
 zsm=10
 zsp=20
  end start
end data
end
```